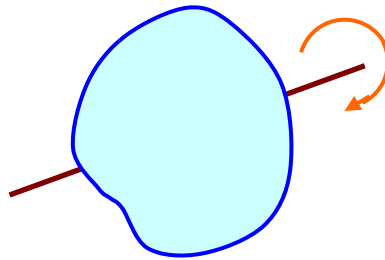


Flow Structure in a Precessing Sphere

Shigeo Kida (Kyoto University)

S. Goto, N. Ishii, M. Nishioka, K. Nakayama, N. Honda

Flow in a Rotating Container



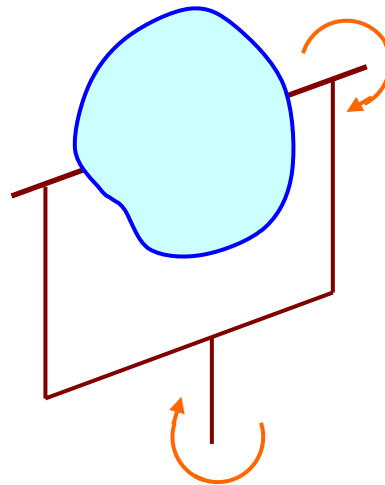
Spin rotation

Flow structure is simple.

Solid-body rotation

It can be proved from NS equation.

Flow in a Precessing Container



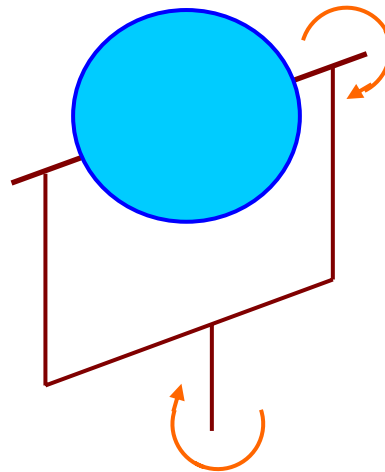
Spin rotation

Precession rotation

Flow structure is non-trivial.

Flow can be turbulent.

Flow in a Precessing Sphere



Spin rotation

Precession rotation

Flow structure is non-trivial.

Flow can be turbulent.

Outline

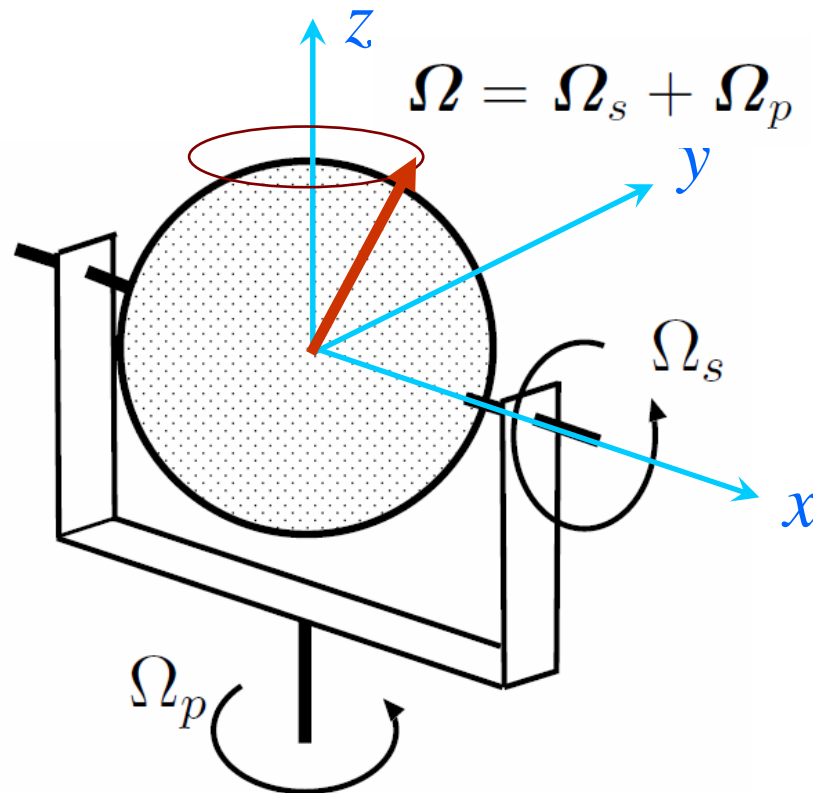
- 1 . Introduction
- 2 . Experiment – State Diagram
- 3 . Numerical Simulation – Stability boundary
Flow Structure
- 4 . Asymptotic Analysis – Flow Structure
- 5 . Summary

Outline

- 1 . Introduction
- 2 . Experiment – State Diagram
- 3 . Numerical Simulation – Stability boundary
Flow Structure
- 4 . Asymptotic Analysis – Flow Structure
- 5 . Summary

Precessing Sphere

We consider the motion of an incompressible viscous fluid in a precessing sphere, where the spin angular velocity Ω_s and the precession angular velocity Ω_p are perpendicular to each other.



Research on Precessing Sphere/Spheroid/Spherical Shell

Precession of the Earth

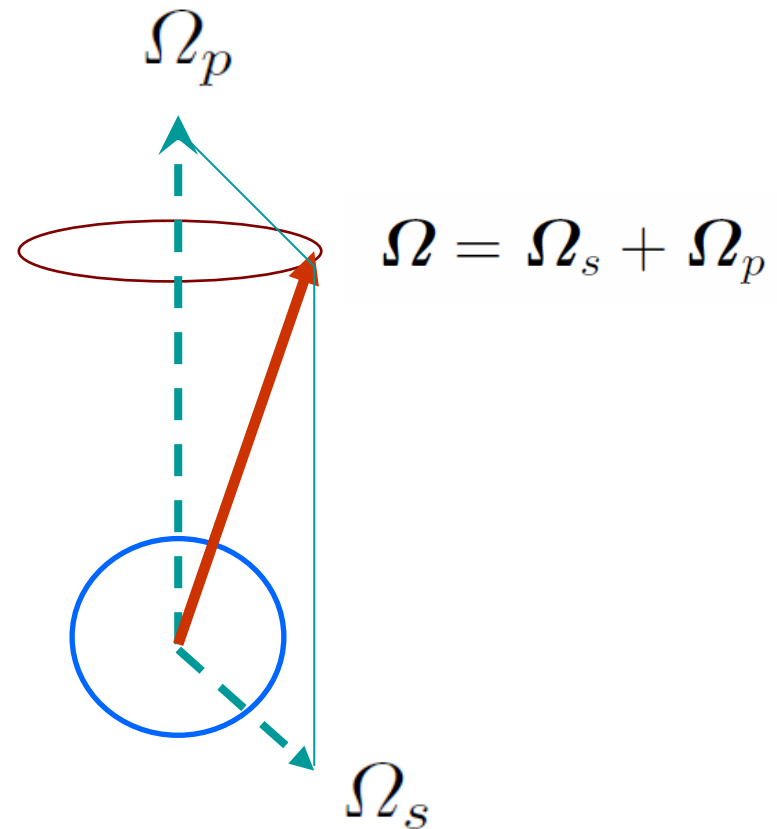
Spin rotation; one day

Precession rotation: 25800 year

Poincare number; 10^{-7}

Precession angle; -23.5°

Ekman number; $10^{-15} < E < 10^{-7}$



Research on Precessing Sphere/Spheroid/Spherical Shell

related to **Geodynamo**

Experiment

Vanyo et al. 1995: Experiments on precessing flows in the Earth's liquid core

Vanyo & Dunn 2000: Core precession: flow structures and energy

Numerical

Lorenzani & Tilgner 2001: Fluid instabilities in precessing spheroidal cavities

Tilgner & Busse 2001: Fluid flows in precessing spherical shells

Tilgner 2005: Precession driven dynamos

Our Motivation

[1] to make a compact turbulence generator

[2] to understand the flow dynamics as one of the standard systems

[3] to contribute to geophysics such as geodynamo

Outline

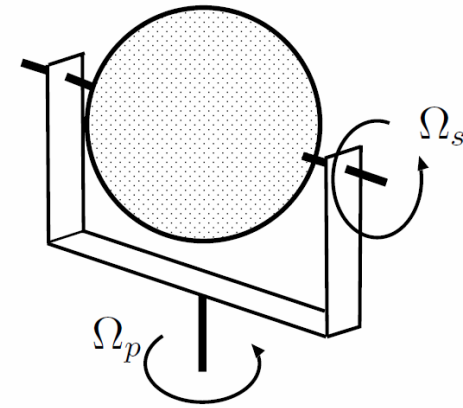
- 1 . Introduction
- 2 . Experiment – State Diagram
- 3 . Numerical Simulation – Stability boundary
Flow Structure
- 4 . Asymptotic Analysis – Flow Structure
- 5 . Summary

Apparatus

Acrylic Sphere + water
($\phi 100\text{mm}$)

Spin axis

Precession axis



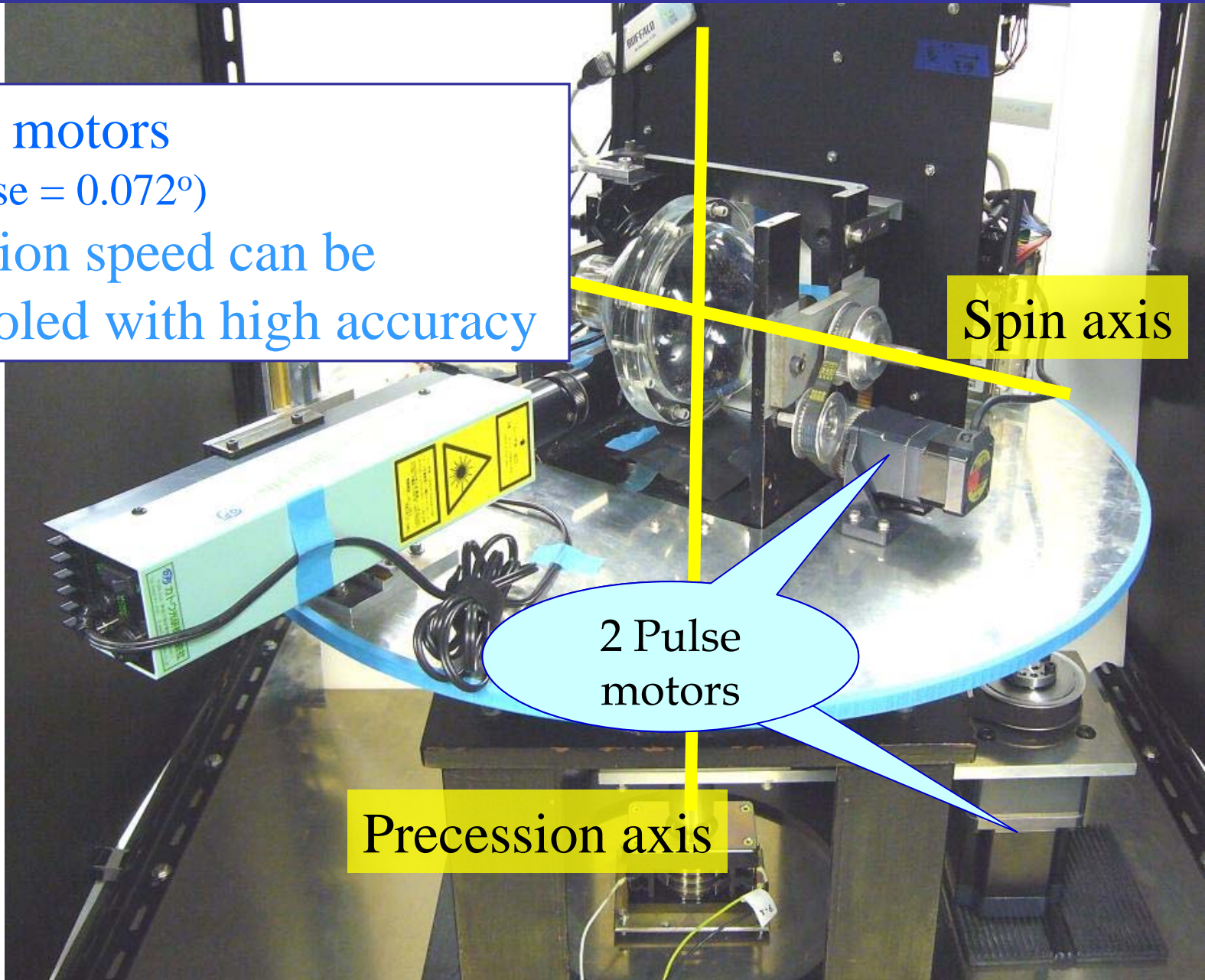
Control of rotation speed

Pulse motors
(1 pulse = 0.072°)
Rotation speed can be
controlled with high accuracy

Spin axis

2 Pulse
motors

Precession axis



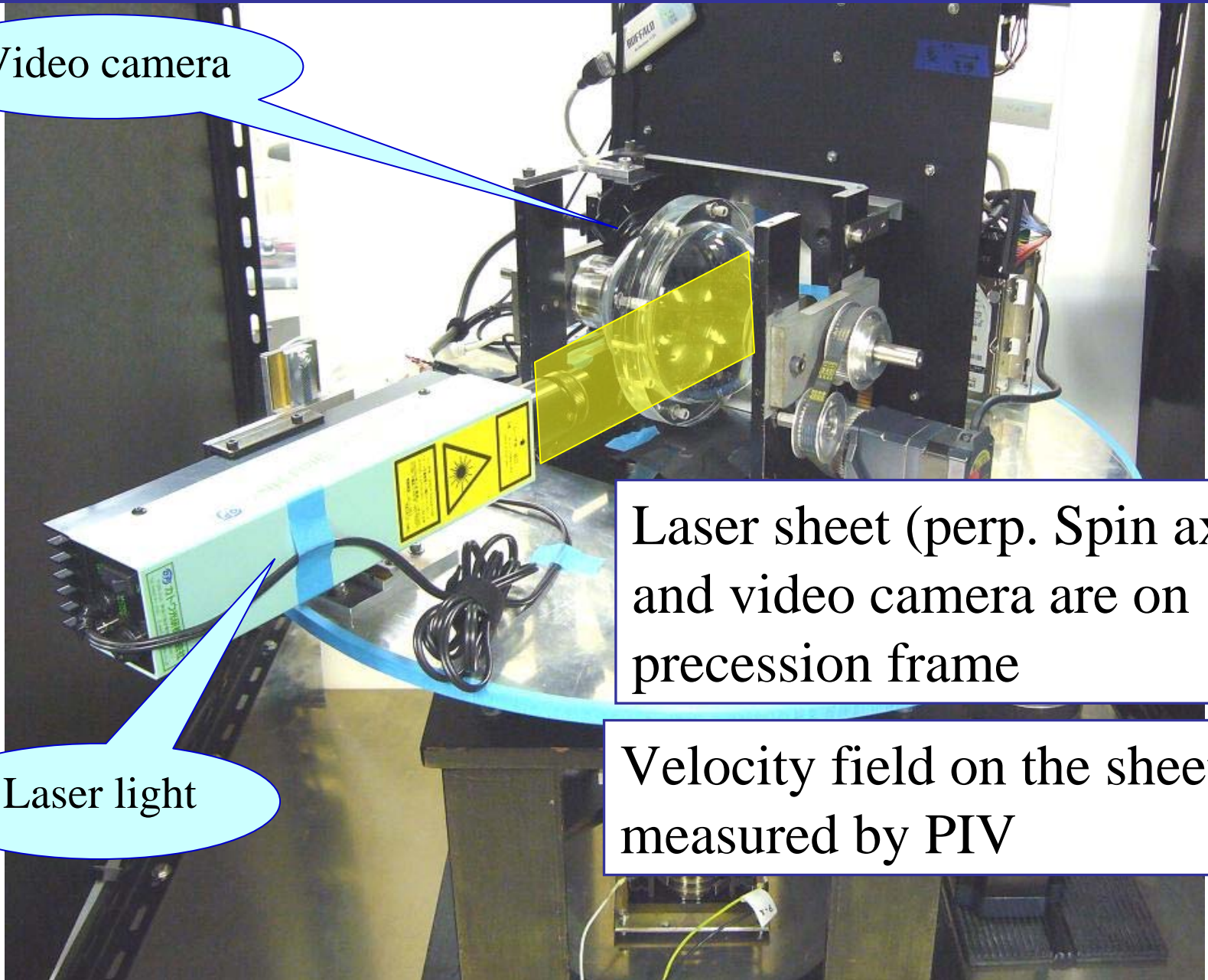
Visualization / Measurement

Video camera

Laser sheet (perp. Spin axis)
and video camera are on
precession frame

Laser light

Velocity field on the sheet is
measured by PIV



Governing Equations (in Precession frame)

$$\frac{\partial \mathbf{u}}{\partial t} = \mathbf{u} \times \boldsymbol{\omega} - 2 \frac{R_p}{R_s} \hat{\mathbf{z}} \times \mathbf{u} - \nabla P + \frac{1}{R_s} \nabla^2 \mathbf{u}$$

Non-dimensional

$$P = p + \frac{1}{2} |\mathbf{u}|^2 - \left(\frac{R_p}{R_s} \right)^2 \frac{1}{2} (\mathbf{r} \times \hat{\mathbf{z}})^2$$

Modified pressure

$$\nabla \cdot \mathbf{u} = 0$$

b. c.

$$\mathbf{u} = \hat{\mathbf{x}} \times \mathbf{r} \quad \text{on } |\mathbf{r}| = 1$$

Control Parameters

Spin Reynolds number

(Reciprocal of Ekman number)

$$R_s = \frac{a^2 \Omega_s}{\nu}$$

Precession Reynolds number

$$R_p = \frac{a^2 \Omega_p}{\nu}$$

When $a=5\text{cm}$, $\nu=0.01 \text{ cm}^2/\text{s}$, $\Omega_s=2\pi n$,

$$R_s = 1.6 \times 10^4 n$$

Control Parameters

Reynolds number

$$Re = \frac{a^2 \Omega_s}{\nu} \quad (\equiv R_s)$$

Poincare number

$$\Gamma = \frac{\Omega_p}{\Omega_s} \quad \left(\equiv \frac{R_p}{R_s} \right)$$

Visualized Flow

$$Re=15,000$$

$$\Gamma=0.00625$$

Solid –body rotation

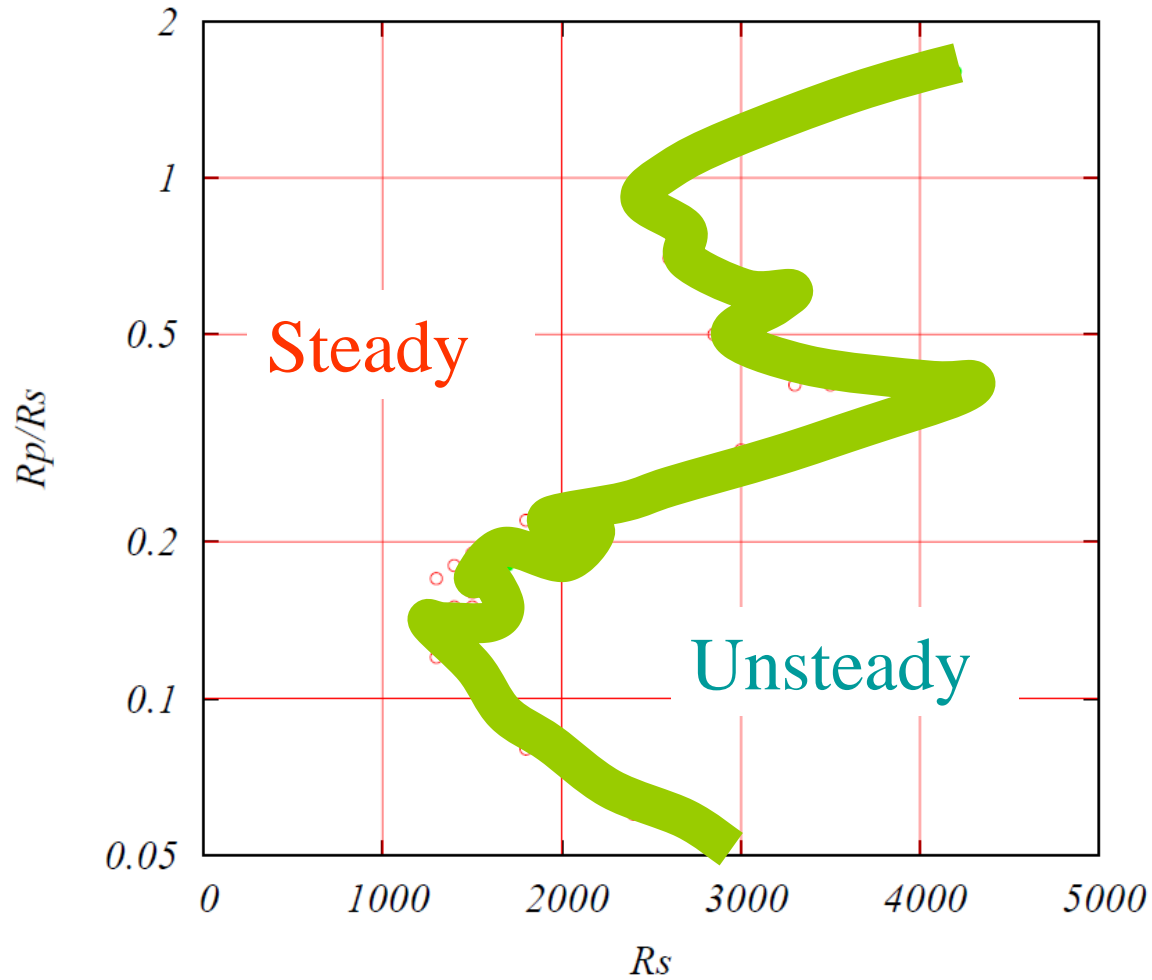
Flow in a Rotating Container

$$Re=15,000$$

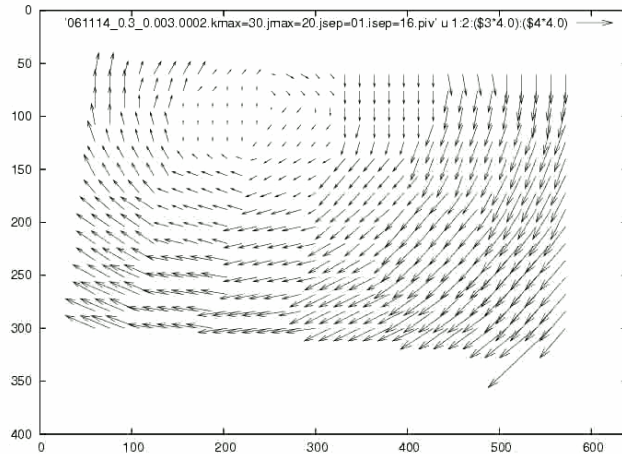
$$\Gamma=0.1$$

Turbulent state

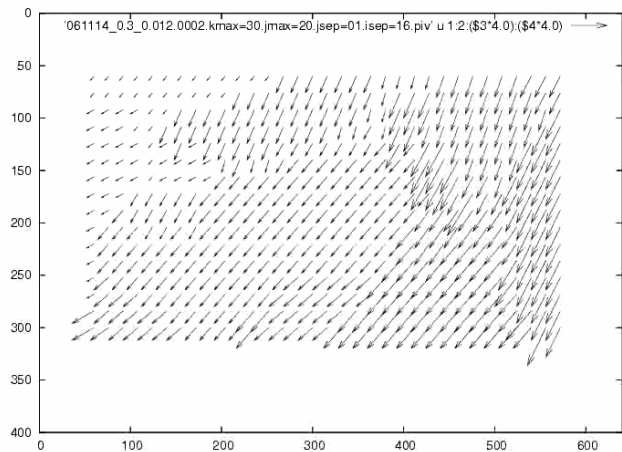
Stability Boundary



Velocity Field (animation)

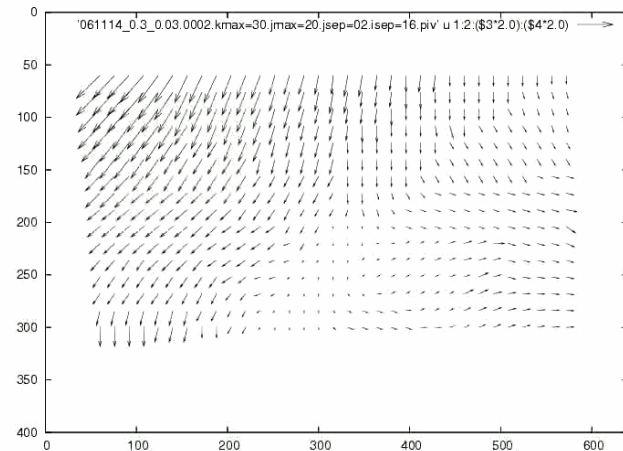


Steady: $R_p/R_s = 0.01$



Periodic: $R_p/R_s = 0.04$

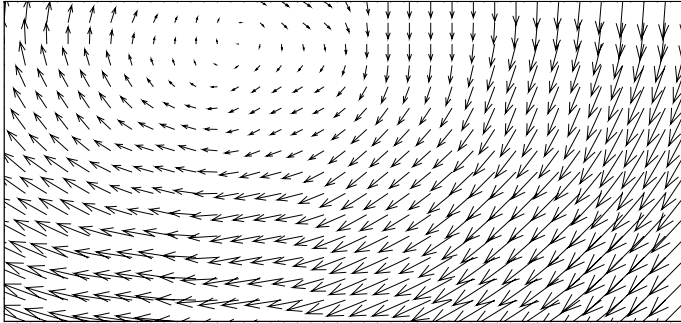
$$R_s \approx 4,500$$



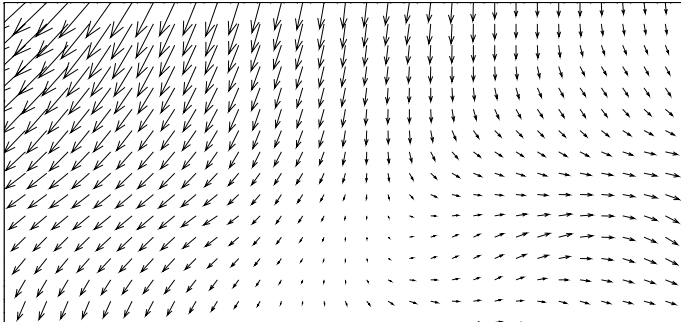
Aperiodic: $R_p/R_s = 0.1$

Velocity Field (snap)

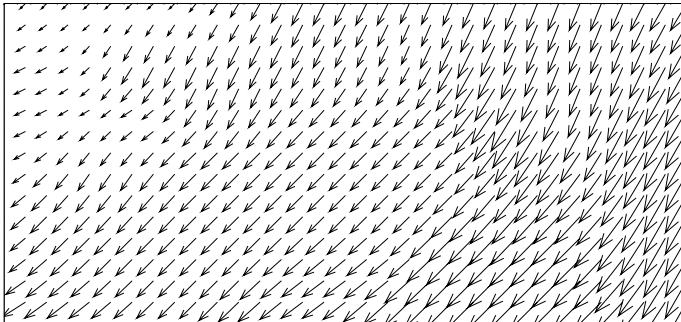
$$R_s \approx 4,500$$



Steady: $R_p/R_s = 0.01$



Periodic: $R_p/R_s = 0.04$



Aperiodic: $R_p/R_s = 0.1$

Judged from two-time correlation function

Two-Time Correlation of Velocity

$$C_i(\mathbf{x}, \tau) = \frac{\langle [u_i(\mathbf{x}, t) - m_i(\mathbf{x})][u_i(\mathbf{x}, t + \tau) - m_i(\mathbf{x})] \rangle}{\sigma_i(\mathbf{x})^2}$$

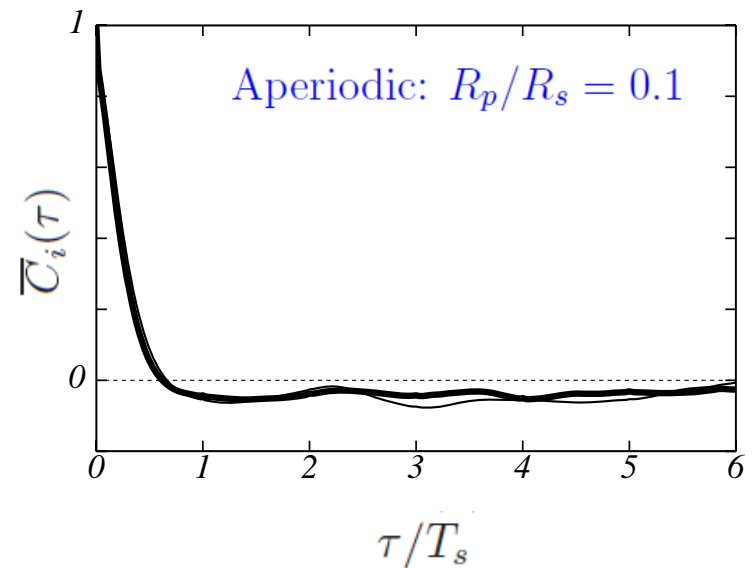
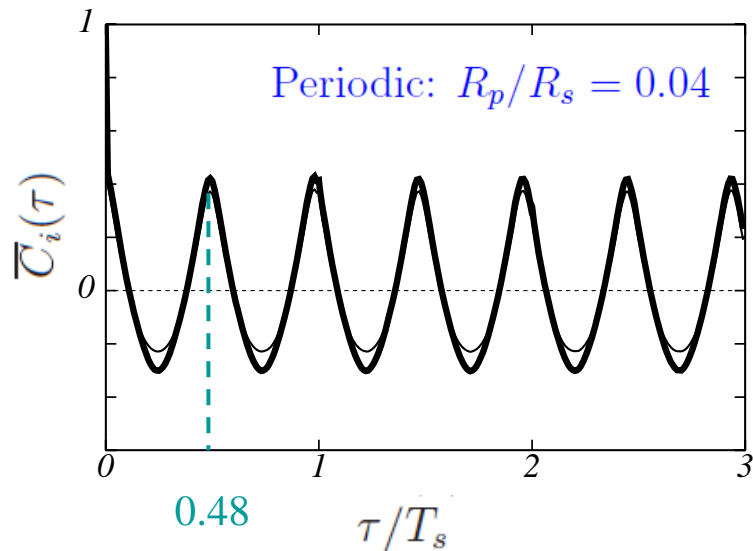
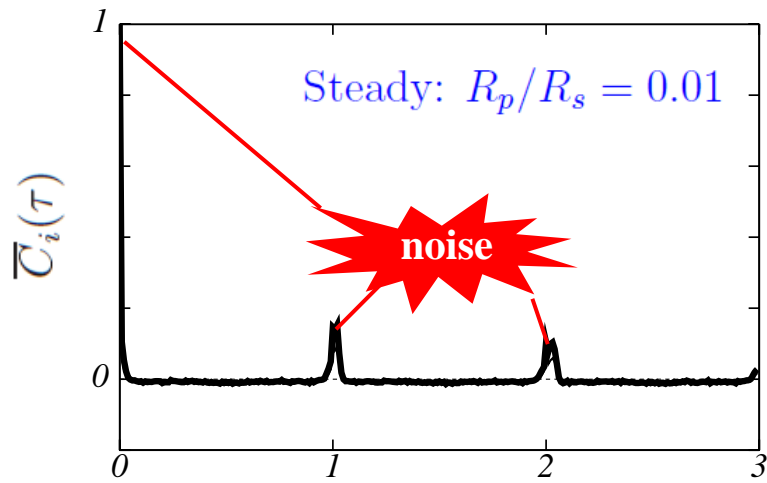
$$(i = 1, 2)$$

$$m_i(\mathbf{x}) = \langle u_i(\mathbf{x}, t) \rangle$$

$$\sigma_i(\mathbf{x})^2 = \langle (u_i(\mathbf{x}, t))^2 \rangle - m_i(\mathbf{x})^2$$

Two-Time Correlation of Velocity

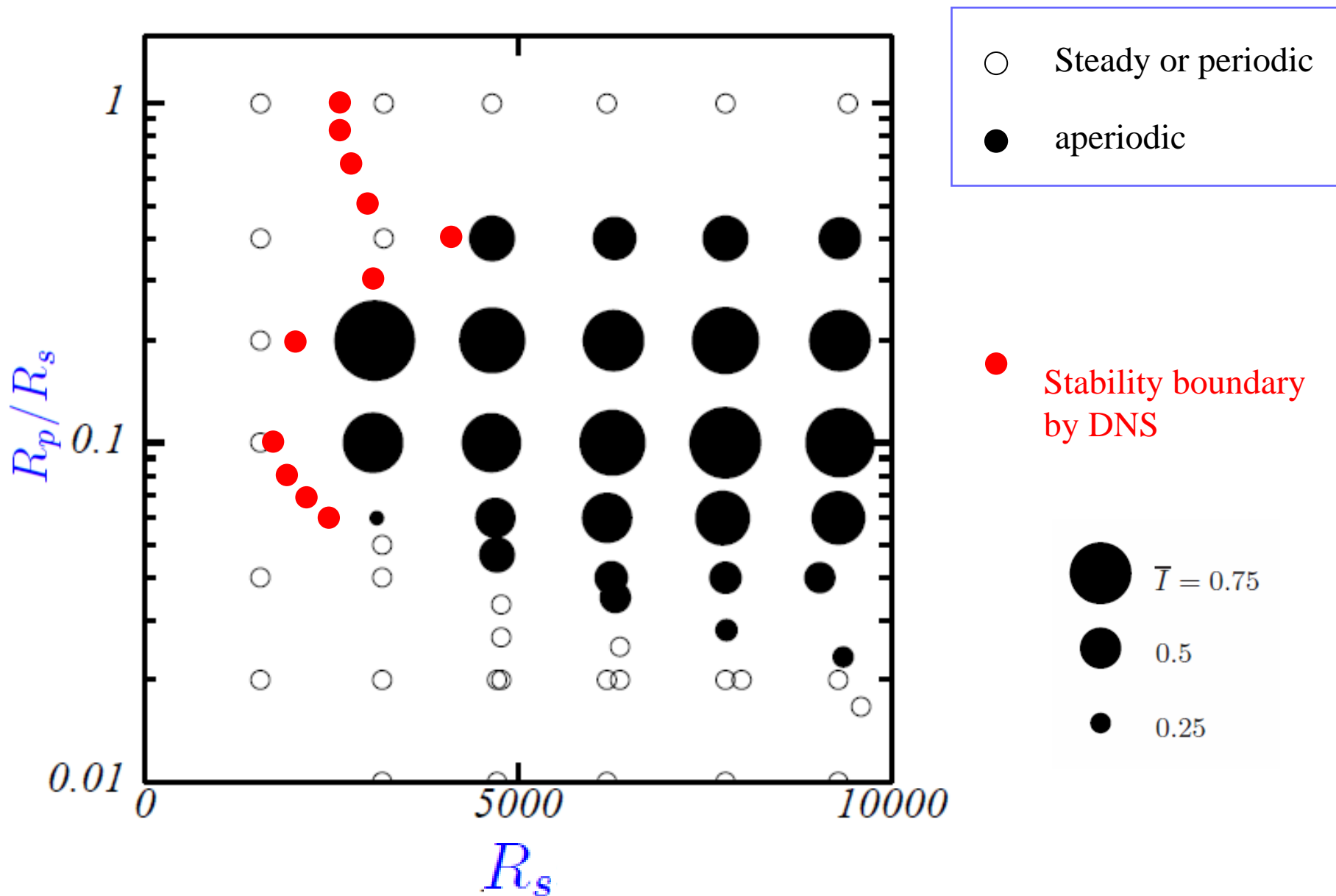
$R_s \approx 4,500$



Fluctuation Magnitude

$$I(\mathbf{x}) = \sqrt{\frac{\langle |\mathbf{u}(\mathbf{x}, t) - \langle \mathbf{u}(\mathbf{x}, t) \rangle|^2 \rangle}{\langle |\mathbf{u}(\mathbf{x}, t)|^2 \rangle}}$$

Fluctuation Magnitude



Outline

- 1 . Introduction
- 2 . Experiment – State Diagram
- 3 . Numerical Simulation – Stability boundary
Flow Structure
- 4 . Asymptotic Analysis – Flow Structure
- 5 . Summary

Stability of Steady Flows

By DNS

Governing Equations (in Precession frame)

$$\frac{\partial \mathbf{u}}{\partial t} = \mathbf{u} \times \boldsymbol{\omega} - 2 \frac{R_p}{R_s} \hat{\mathbf{z}} \times \mathbf{u} - \nabla P + \frac{1}{R_s} \nabla^2 \mathbf{u}$$

$$\nabla \cdot \mathbf{u} = 0$$

b. c.

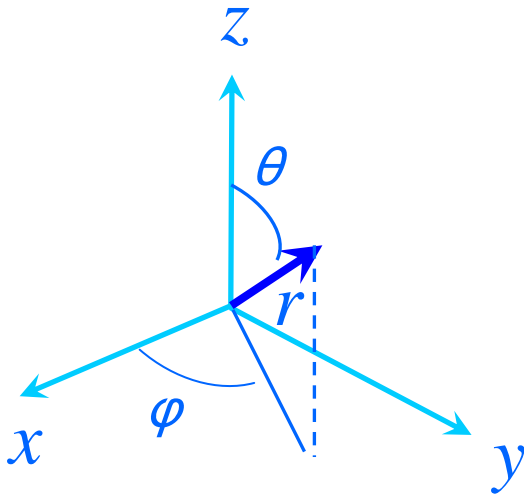
$$\mathbf{u} = \hat{\mathbf{x}} \times \mathbf{r} \quad \text{on } |\mathbf{r}| = 1$$

Poloidal / Toroidal Representation

① Incompressible (solenoidal)

② Spherical geometry

$$\mathbf{u} = \nabla \times (\nabla \times (rU)) + \nabla \times (rW)$$



$$u_r = -\frac{1}{r} \nabla_{\perp}^2 U,$$

$$u_{\theta} = \frac{1}{r} \frac{\partial^2 (rU)}{\partial r \partial \theta} + \frac{1}{\sin \theta} \frac{\partial W}{\partial \varphi},$$

$$u_{\varphi} = \frac{1}{r \sin \theta} \frac{\partial^2 (rU)}{\partial r \partial \varphi} - \frac{\partial W}{\partial \theta}$$

Vorticity

$$\boldsymbol{\omega} = \nabla \times \nabla \times (\mathbf{r}W) + \nabla \times (\mathbf{r}(-\nabla^2 U))$$

$$\omega_r = -\frac{1}{r} \nabla_{\perp}^2 W$$

$$\omega_{\theta} = \frac{1}{r} \frac{\partial^2 (rW)}{\partial r \partial \theta} + \frac{1}{\sin \theta} \frac{\partial}{\partial \varphi} (-\nabla^2 U)$$

$$\omega_{\varphi} = \frac{1}{r \sin \theta} \frac{\partial^2 (rW)}{\partial r \partial \varphi} - \frac{\partial}{\partial \theta} (-\nabla^2 U)$$

Governing Equations (in Precession frame)

$$\frac{\partial \mathbf{u}}{\partial t} = \mathbf{u} \times \boldsymbol{\omega} - 2 \frac{R_p}{R_s} \hat{\mathbf{z}} \times \mathbf{u} - \nabla P + \frac{1}{R_s} \nabla^2 \mathbf{u}$$

$$\nabla \cdot \mathbf{u} = 0$$

b. c.

$$\mathbf{u} = \hat{\mathbf{x}} \times \mathbf{r} \quad \text{on } |\mathbf{r}| = 1$$

Poloidal / Toroidal Equations

$$\begin{aligned}
 & -\nabla_{\perp}^2 \left(\nabla^2 - R_h \frac{\partial}{\partial t} \right) W \\
 = & -2R_v \left[\frac{\partial W}{\partial \varphi} + \frac{1}{r^2} \left\{ \nabla_{\perp}^2 \left(r \sin \theta \frac{\partial}{\partial \theta} - r \frac{\partial}{\partial r} r \cos \theta \right) - r \frac{\partial}{\partial r} \left(r \sin \theta \frac{\partial}{\partial \theta} + 2r \cos \theta \right) \right\} U \right] \\
 & + \frac{R_h}{r^2 \sin^2 \theta} \left[\frac{\partial}{\partial \varphi} (r^2 \sin \theta N_{\theta} - r \sin \theta \frac{\partial}{\partial \theta} (r \sin \theta N_{\varphi})) \right], \quad \boxed{N = u \times \omega}
 \end{aligned}$$

$$\begin{aligned}
 & -\nabla_{\perp}^2 \left(\nabla^2 - R_h \frac{\partial}{\partial t} \right) (-\nabla^2 U) \\
 = & -2R_v \left[\frac{\partial(-\nabla^2 U)}{\partial \varphi} + \frac{1}{r^2} \left\{ \nabla_{\perp}^2 \left(r \sin \theta \frac{\partial}{\partial \theta} - r \frac{\partial}{\partial r} r \cos \theta \right) - r \frac{\partial}{\partial r} \left(r \sin \theta \frac{\partial}{\partial \theta} + 2r \cos \theta \right) \right\} W \right] \\
 & + \frac{R_h}{r^2} \left[\nabla_{\perp}^2 (r N_r) - \frac{1}{r^2 \sin^2 \theta} \left(r \frac{\partial}{\partial r} - 2 \right) r \sin \theta \frac{\partial}{\partial \theta} (r^2 \sin \theta N_{\theta}) - \frac{1}{\sin^2 \theta} r \frac{\partial}{\partial r} \frac{\partial}{\partial \varphi} (r \sin \theta N_{\varphi}) \right]
 \end{aligned}$$

b. c. $U = 0, \quad \frac{\partial U}{\partial r} = 0, \quad W = \sin \theta \cos \varphi \quad \text{on } r = 1$

Numerical Scheme (Time Integration)

$$-\nabla_{\perp}^2 \left(\nabla^2 - R_h \frac{\partial}{\partial t} \right) W = G$$

$$-\nabla_{\perp}^2 \left(\nabla^2 - R_h \frac{\partial}{\partial t} \right) (-\nabla^2 U) = H$$

$$U = 0, \quad \frac{\partial U}{\partial r} = 0, \quad W = \sin \theta \cos \varphi \quad (\text{on } r = 1)$$

Adams-Bashforth / Crank-Nicolson Scheme

$$\Delta t = 2\pi/1000$$

$$-\nabla_{\perp}^2 \left(\nabla^2 - \frac{2R_h}{\Delta t} \right) W^{t+\Delta t} = \nabla_{\perp}^2 \left(\nabla^2 + \frac{2R_h}{\Delta t} \right) W^t + 3G^t - G^{t-\Delta t}$$

$$-\nabla_{\perp}^2 \left(\nabla^2 - \frac{2R_h}{\Delta t} \right) (-\nabla^2) U^{t+\Delta t} = \nabla_{\perp}^2 \left(\nabla^2 + \frac{2R_h}{\Delta t} \right) (-\nabla^2) U^t + 3H^t - H^{t-\Delta t}$$

$$U^{t+\Delta t} = 0, \quad \frac{\partial}{\partial r} U^{t+\Delta t} = 0, \quad W^{t+\Delta t} = \sin \theta \cos \varphi \quad (\text{on } r = 1)$$

Numerical Scheme (Spatial Differentiation)

Fourier – Legendre – Jacobi Expansion

32×42×85

dealiasd

$$U^t(r, \theta, \varphi) = \sum_{l=0}^{N-1} \sum_{m=-l}^l \sum_{j=1}^{[(N-l+1)/2]} \tilde{U}_{jlm}^t \Phi_k^l(r) \check{P}_l^{|m|}(\cos \theta) e^{im\varphi}$$

$$W^t(r, \theta, \varphi) = \sum_{l=0}^{N-1} \sum_{m=-l}^l \sum_{j=1}^{[(N-l+1)/2]} \tilde{W}_{jlm}^t \Phi_k^l(r) \check{P}_l^{|m|}(\cos \theta) e^{im\varphi}$$

$$\frac{1}{r^2} \frac{d}{dr} \left((1 - r^2) r^2 \frac{d}{dr} \right) \Phi_k^l - \frac{l(l+1)}{r^2} \Phi_k^l + k(k+3) \Phi_k^l = 0$$

$(0 \leq r \leq 1, 0 \leq l \leq k, k+l = \text{even})$

Orthogonal Relation $\int_0^1 \Phi_n^l(r) \Phi_{n'}^l(r) r^2 dr = \delta_{nn'}$

Matsushima & Marcus (1995)

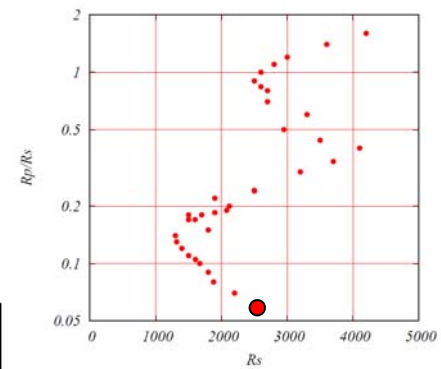
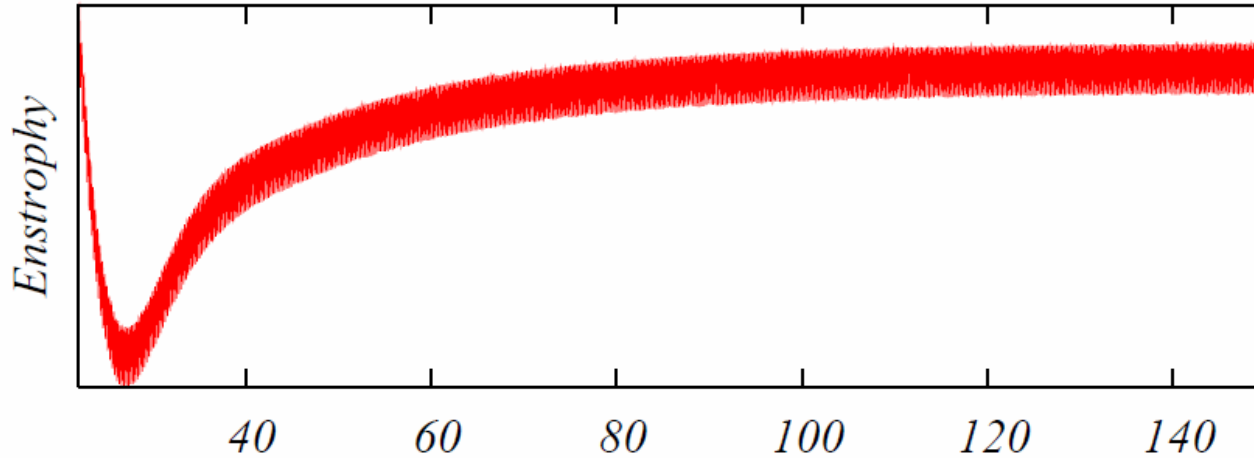
Poloidal / Toroidal Equations

$$\begin{aligned}
 & -\nabla_{\perp}^2 \left(\nabla^2 - R_h \frac{\partial}{\partial t} \right) W \\
 = & -2R_v \left[\frac{\partial W}{\partial \varphi} + \frac{1}{r^2} \left\{ \nabla_{\perp}^2 \left(r \sin \theta \frac{\partial}{\partial \theta} - r \frac{\partial}{\partial r} r \cos \theta \right) - r \frac{\partial}{\partial r} \left(r \sin \theta \frac{\partial}{\partial \theta} + 2r \cos \theta \right) \right\} U \right] \\
 & + \frac{R_h}{r^2 \sin^2 \theta} \left[\frac{\partial}{\partial \varphi} (r^2 \sin \theta N_{\theta} - r \sin \theta \frac{\partial}{\partial \theta} (r \sin \theta N_{\varphi})) \right], \quad \boxed{N = u \times \omega}
 \end{aligned}$$

$$\begin{aligned}
 & -\nabla_{\perp}^2 \left(\nabla^2 - R_h \frac{\partial}{\partial t} \right) (-\nabla^2 U) \\
 = & -2R_v \left[\frac{\partial(-\nabla^2 U)}{\partial \varphi} + \frac{1}{r^2} \left\{ \nabla_{\perp}^2 \left(r \sin \theta \frac{\partial}{\partial \theta} - r \frac{\partial}{\partial r} r \cos \theta \right) - r \frac{\partial}{\partial r} \left(r \sin \theta \frac{\partial}{\partial \theta} + 2r \cos \theta \right) \right\} W \right] \\
 & + \frac{R_h}{r^2} \left[\nabla_{\perp}^2 (r N_r) - \frac{1}{r^2 \sin^2 \theta} \left(r \frac{\partial}{\partial r} - 2 \right) r \sin \theta \frac{\partial}{\partial \theta} (r^2 \sin \theta N_{\theta}) - \frac{1}{\sin^2 \theta} r \frac{\partial}{\partial r} \frac{\partial}{\partial \varphi} (r \sin \theta N_{\varphi}) \right]
 \end{aligned}$$

b. c. $U = 0, \quad \frac{\partial U}{\partial r} = 0, \quad W = \sin \theta \cos \varphi \quad \text{on } r = 1$

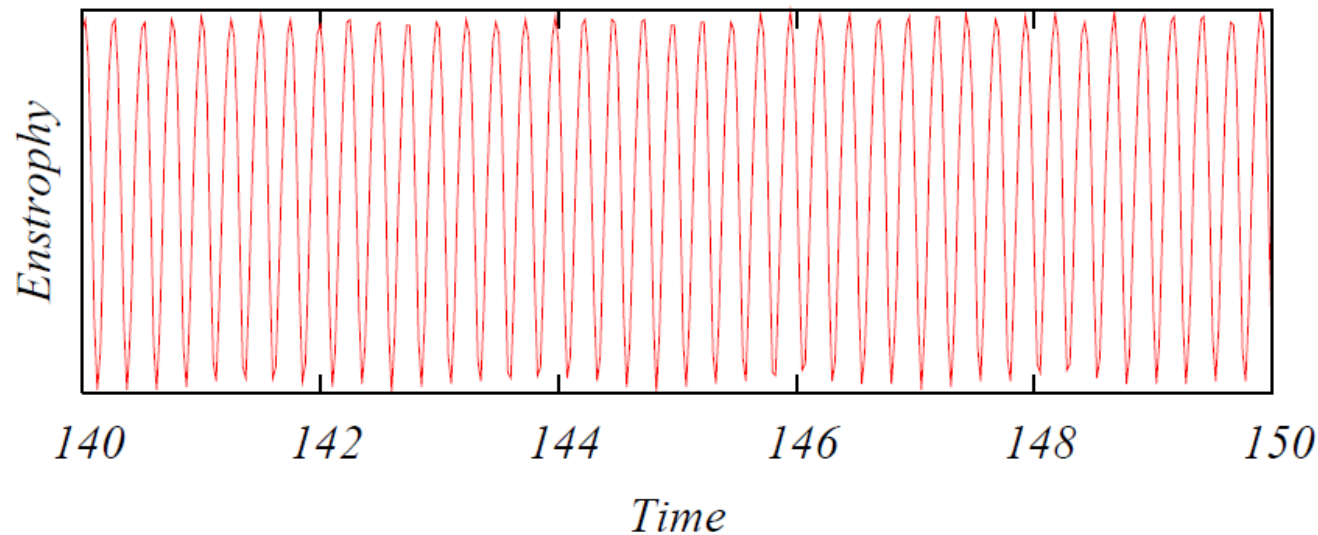
Time-Series of Enstrophy



$$R_s = 2450$$

$$R_p = 147$$

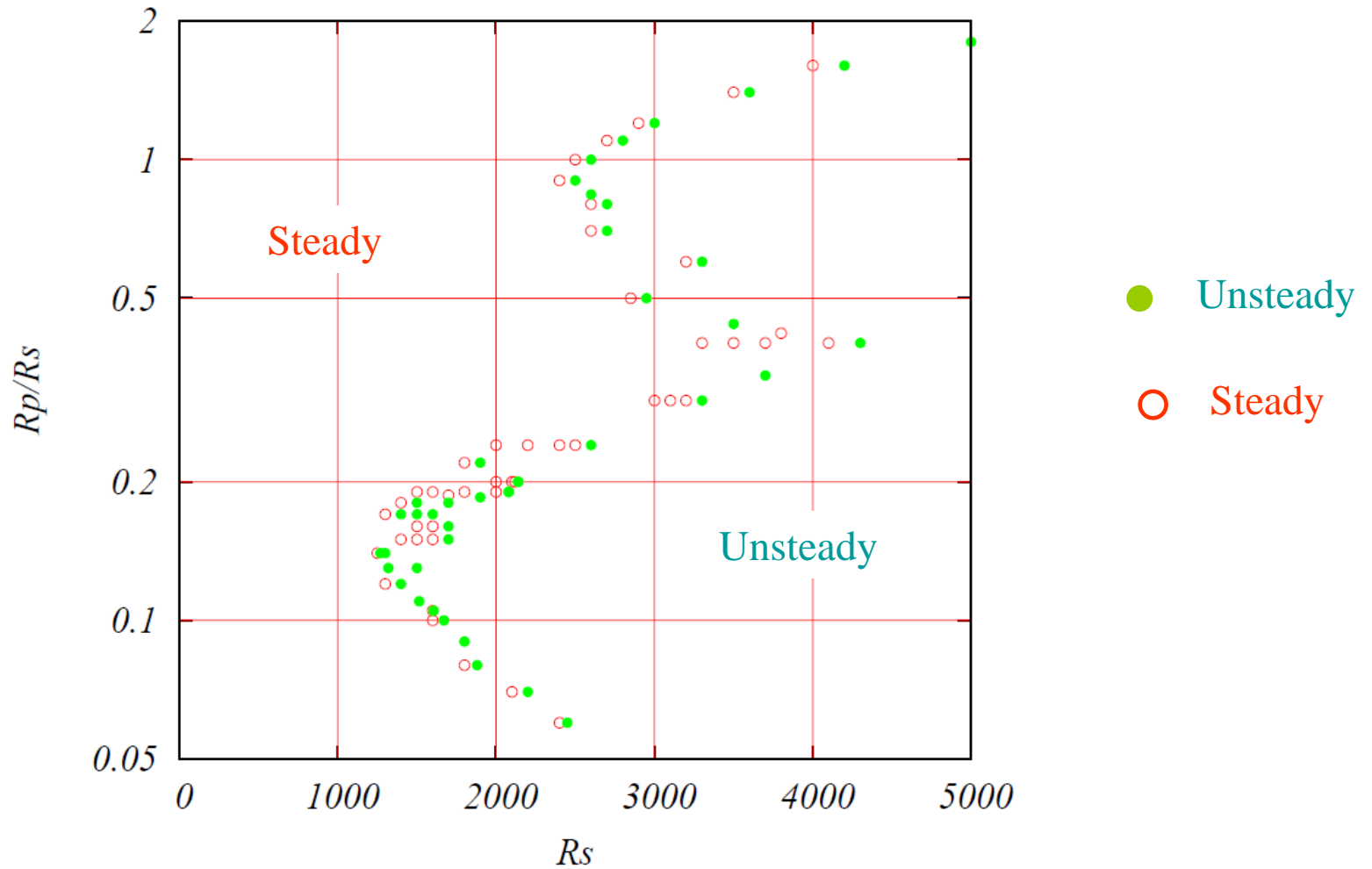
$$\gamma = 0.06$$



$$\lambda = 0.25$$

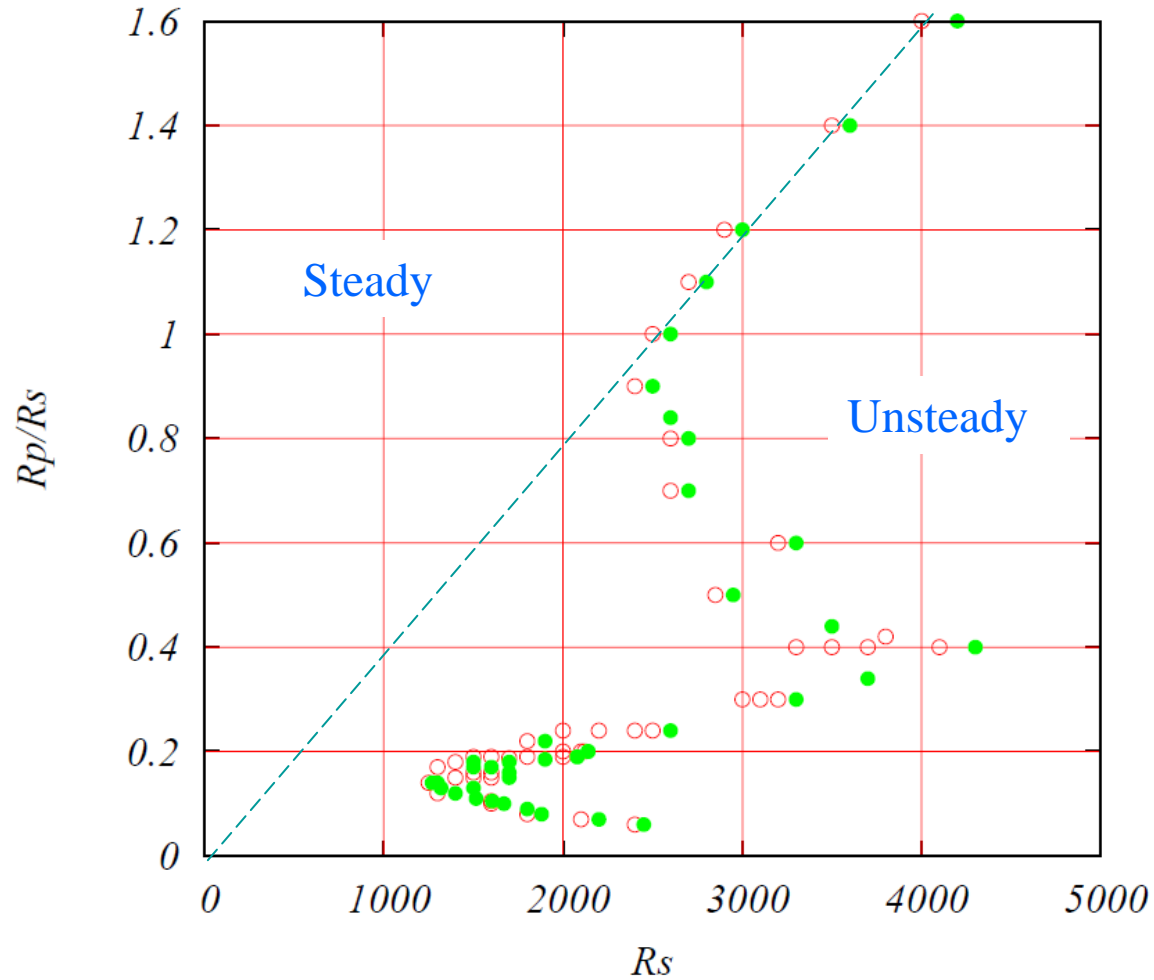
Stability Boundary

in progress

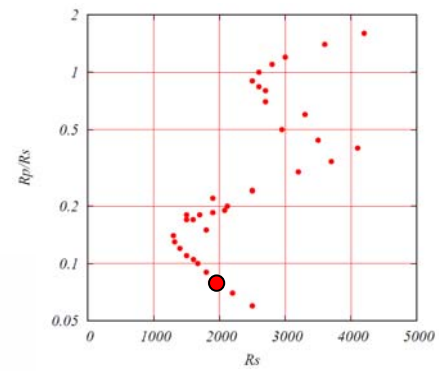


Stability Boundary

in progress



Time-Series of Enstrophy

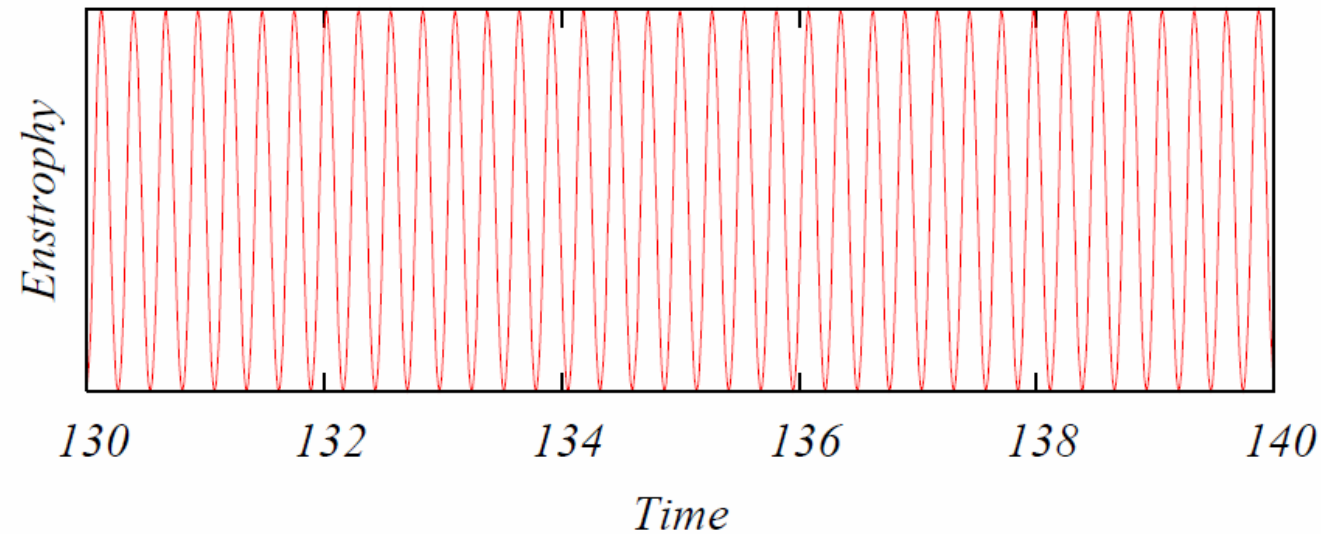
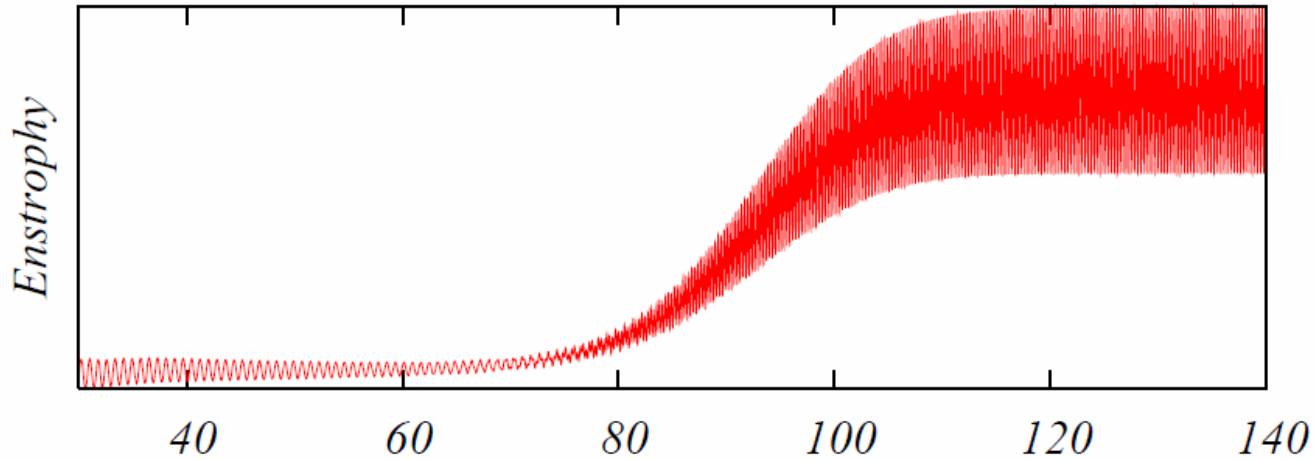


$$R_s = 1880$$

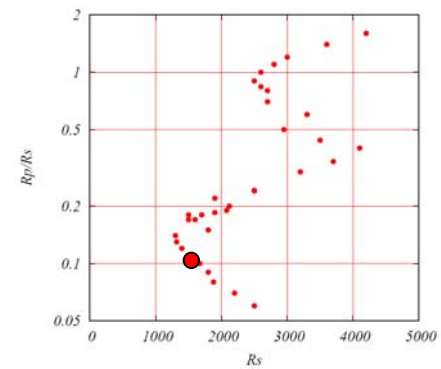
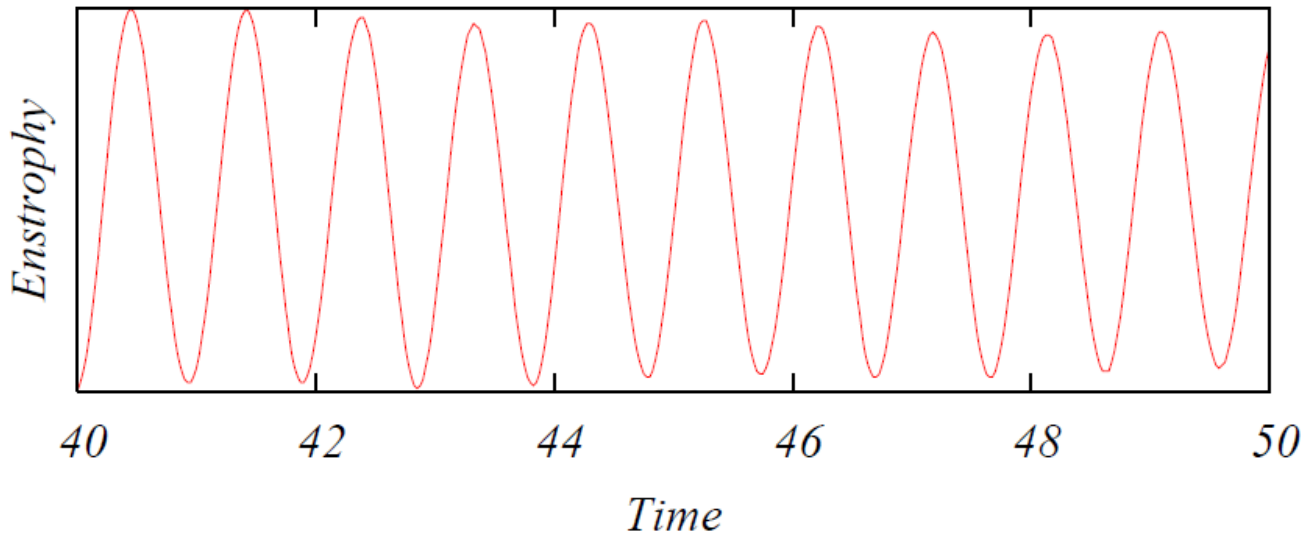
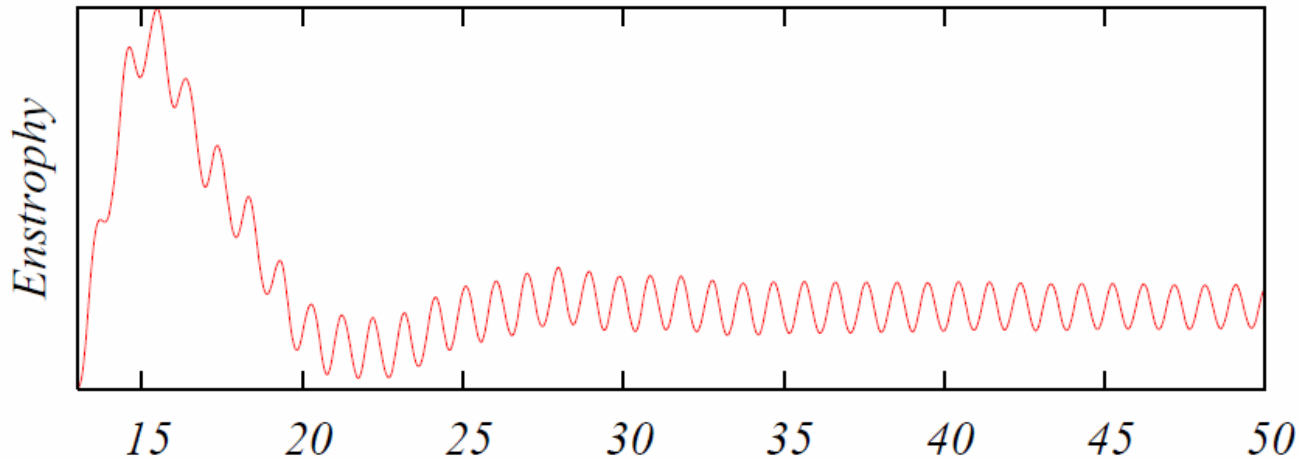
$$R_p = 150.4$$

$$\gamma = 0.08$$

$$\lambda = 0.27$$



Time-Series of Enstrophy



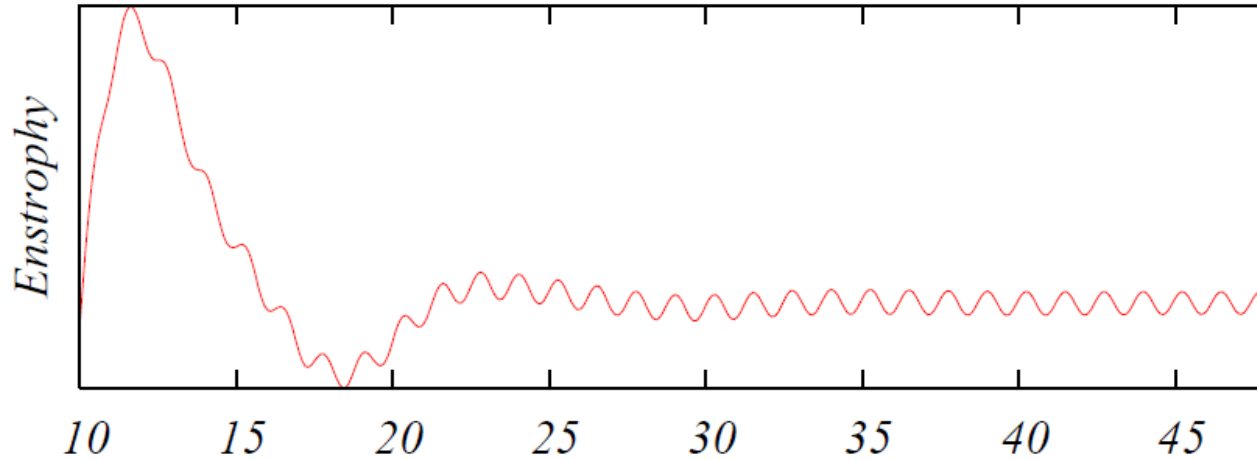
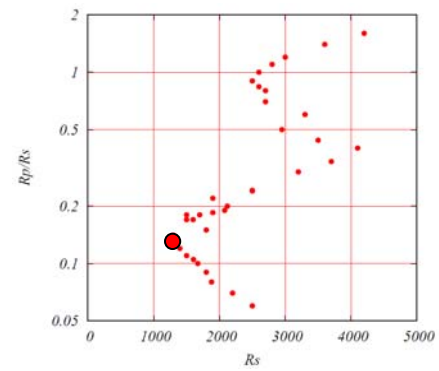
$$R_s = 1515$$

$$R_p = 166.65$$

$$\gamma = 0.11$$

$$\lambda = 0.96$$

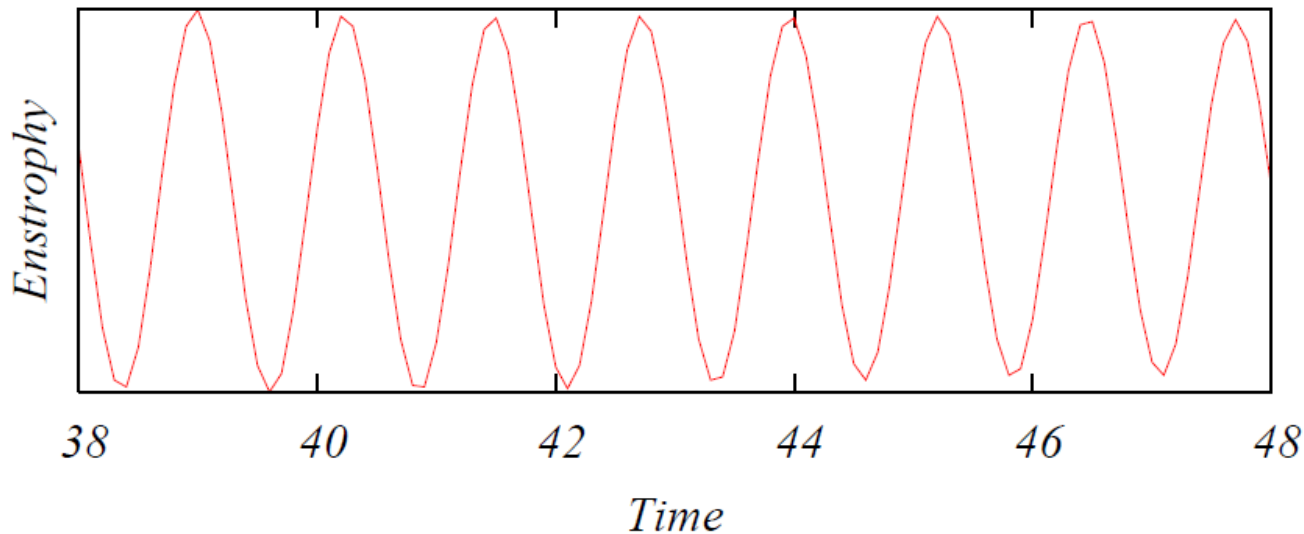
Time-Series of Enstrophy



$$R_s = 1270$$

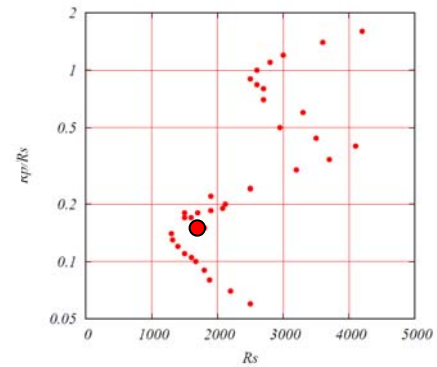
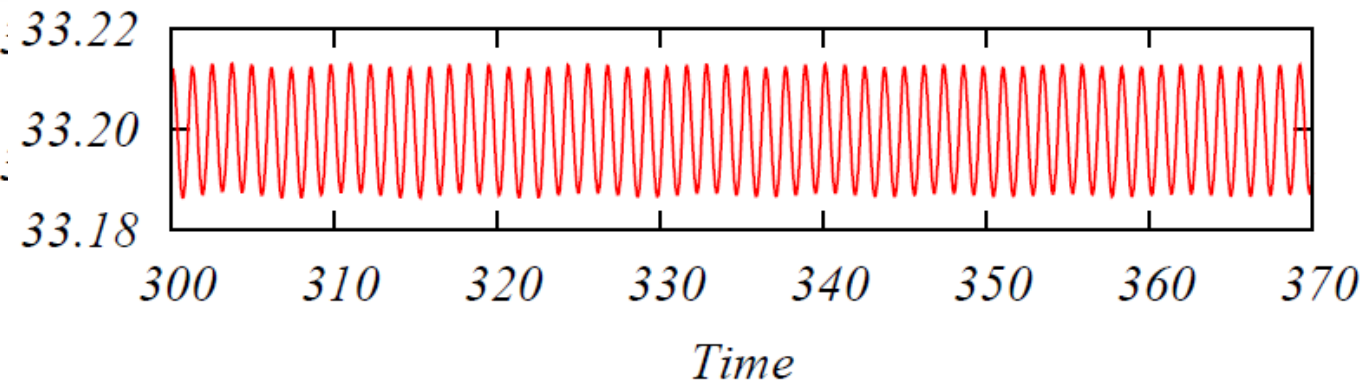
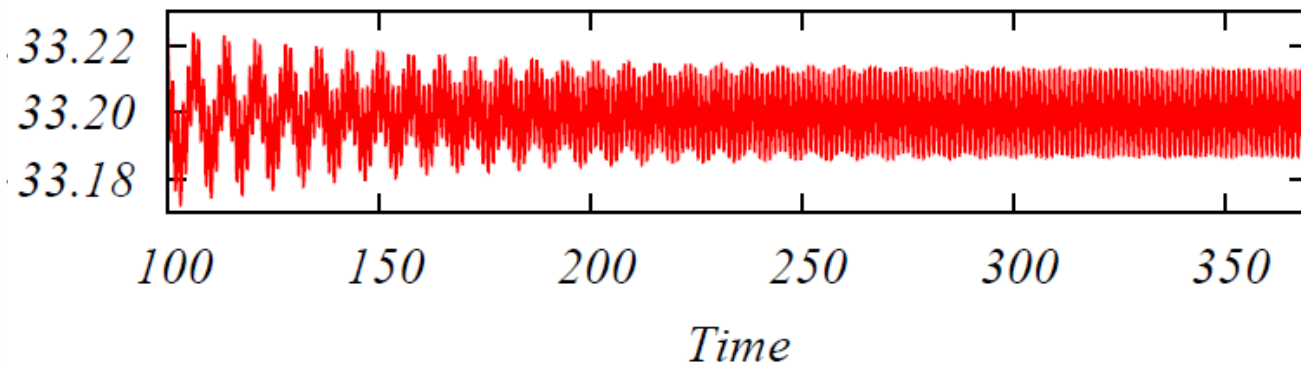
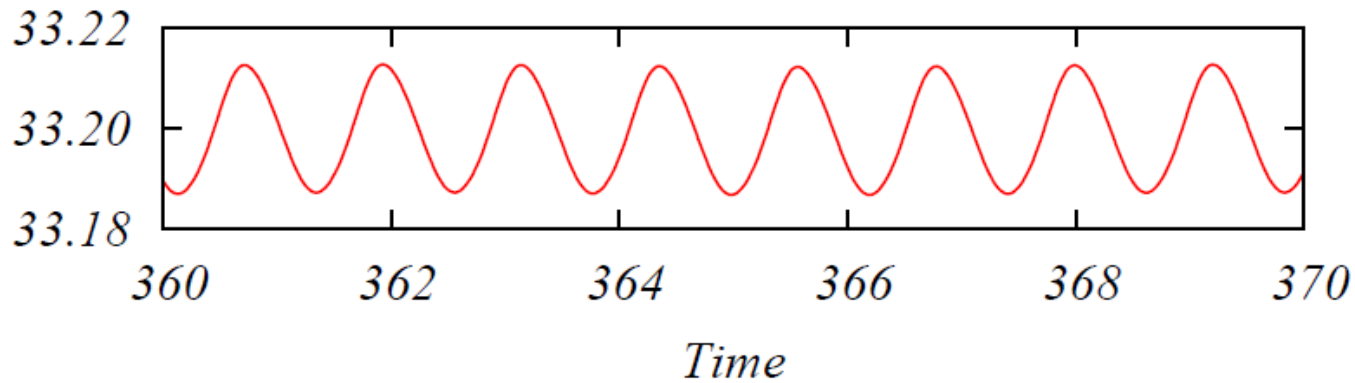
$$R_p = 177.8$$

$$\gamma = 0.14$$



$$\lambda = 1.24$$

Time-Series of Enstrophy



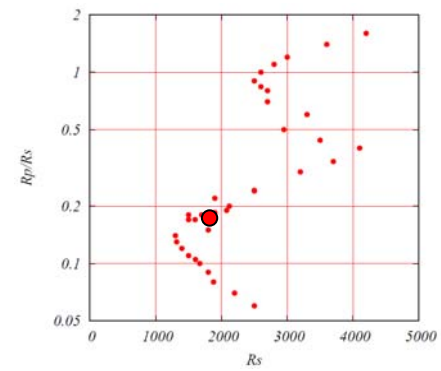
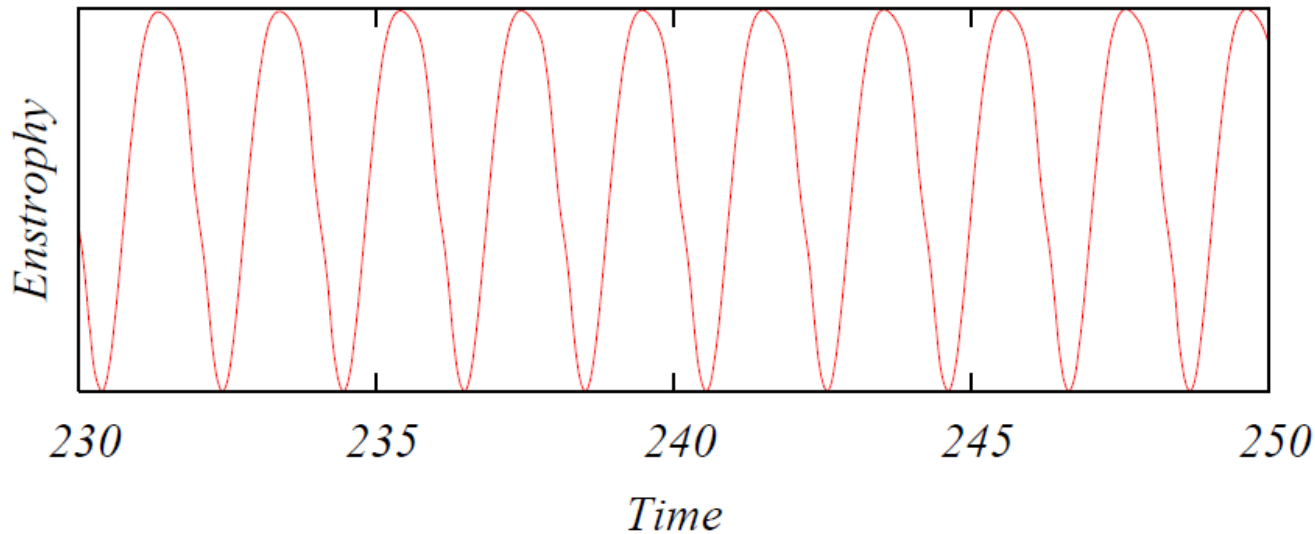
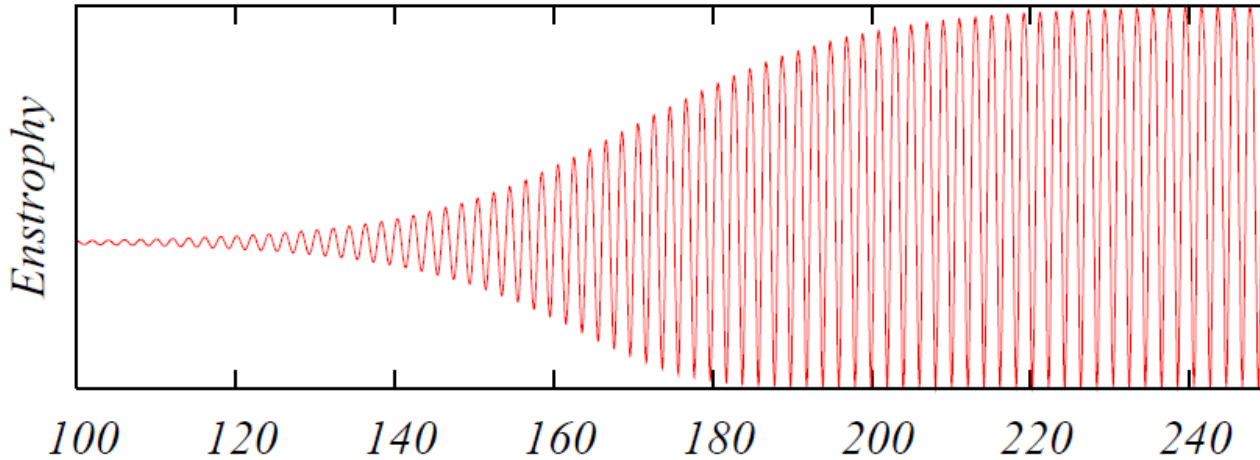
$$R_s = 1700$$

$$R_p = 255$$

$$\gamma = 0.15$$

$$\lambda = 1.21$$

Time-Series of Enstrophy



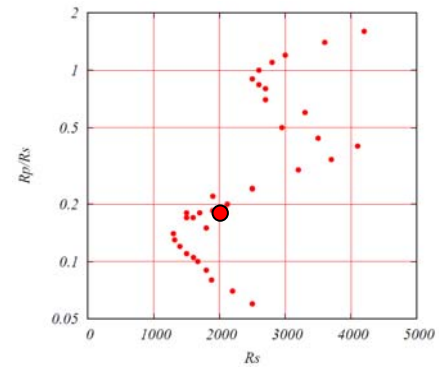
$$R_s = 1900$$

$$R_p = 351.5$$

$$\gamma = 0.185$$

$$\lambda = 2.03$$

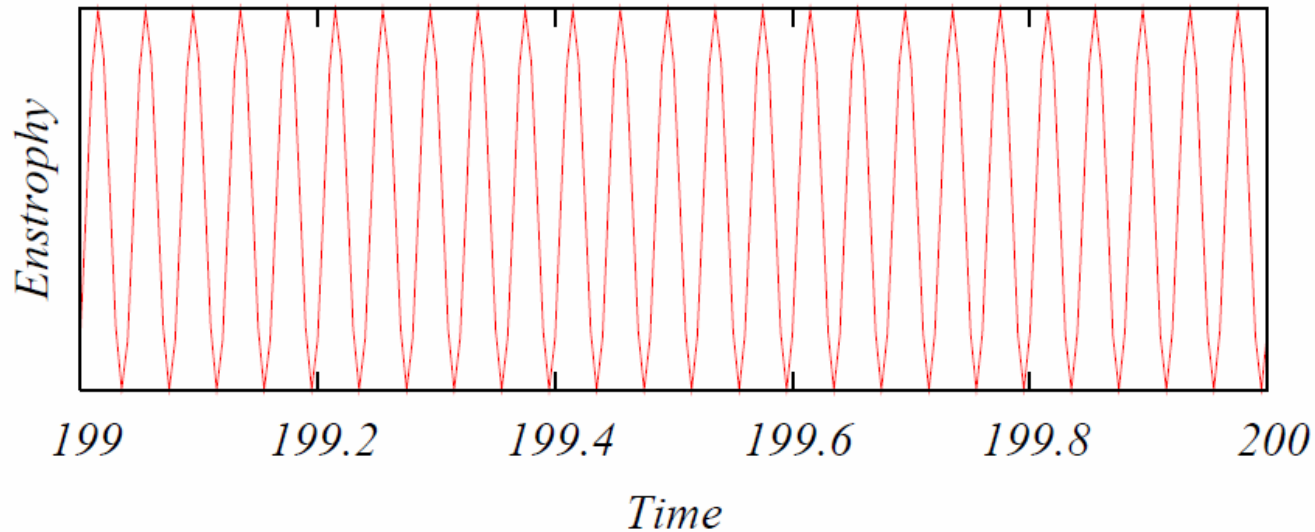
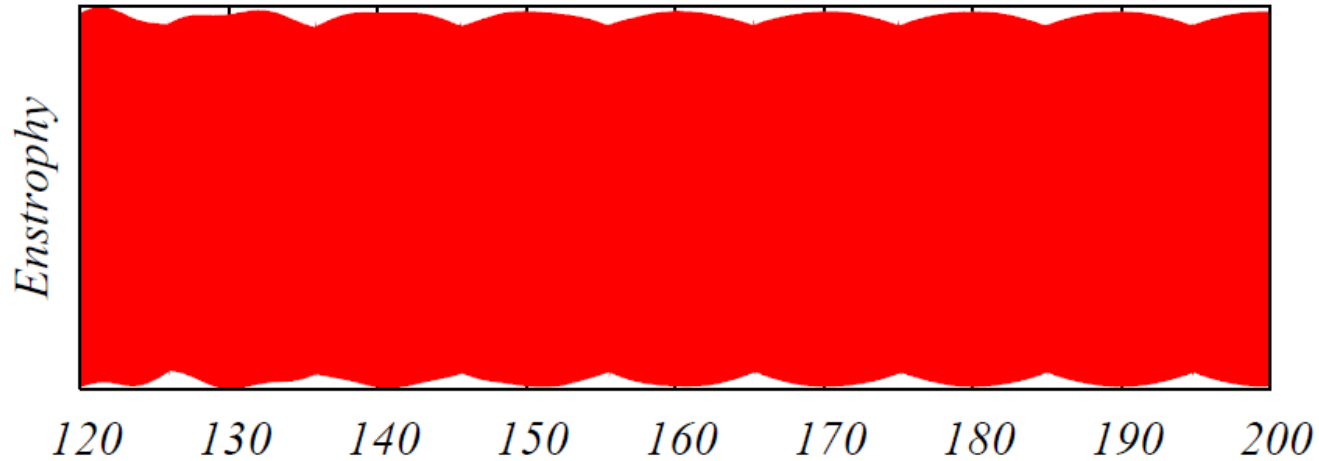
Time-Series of Enstrophy



$$R_s = 2080$$

$$R_p = 395.2$$

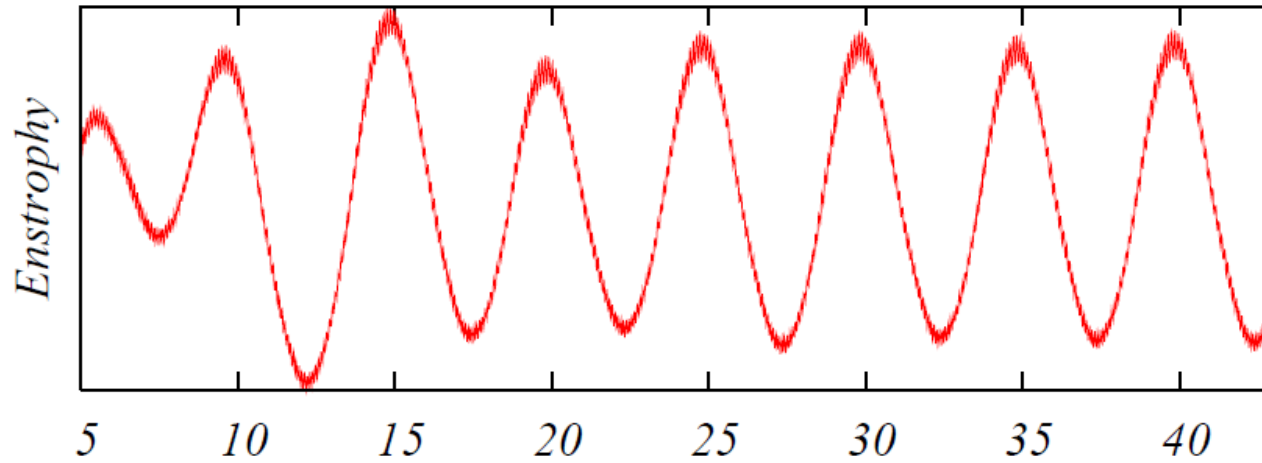
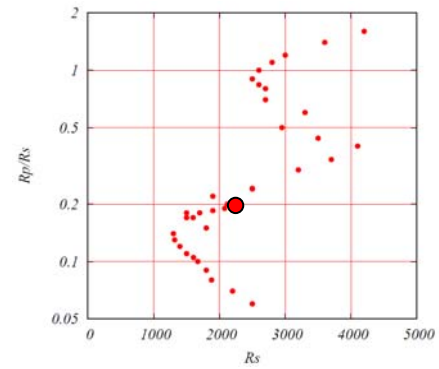
$$\gamma = 0.19$$



$$\lambda = 10.0$$

$$\lambda = 0.04$$

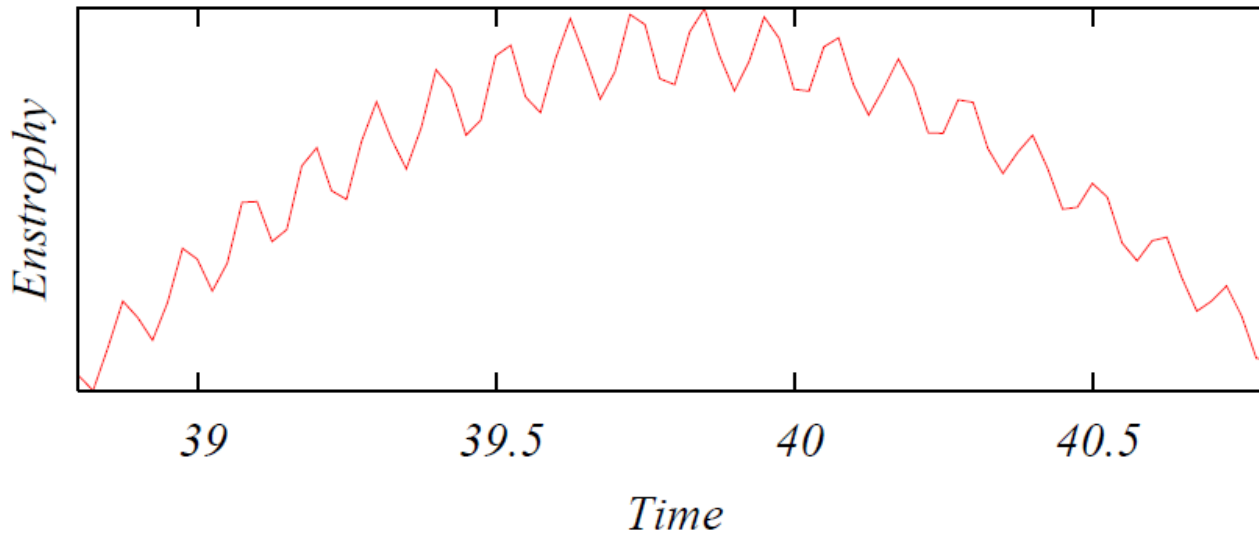
Time-Series of Enstrophy



$$R_s = 2140$$

$$R_p = 428$$

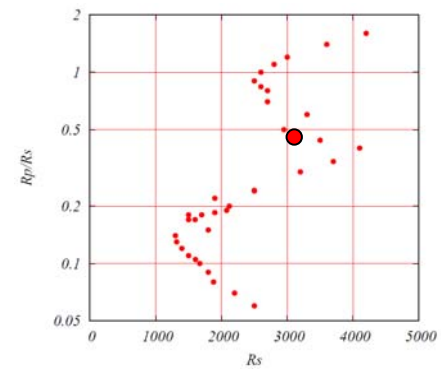
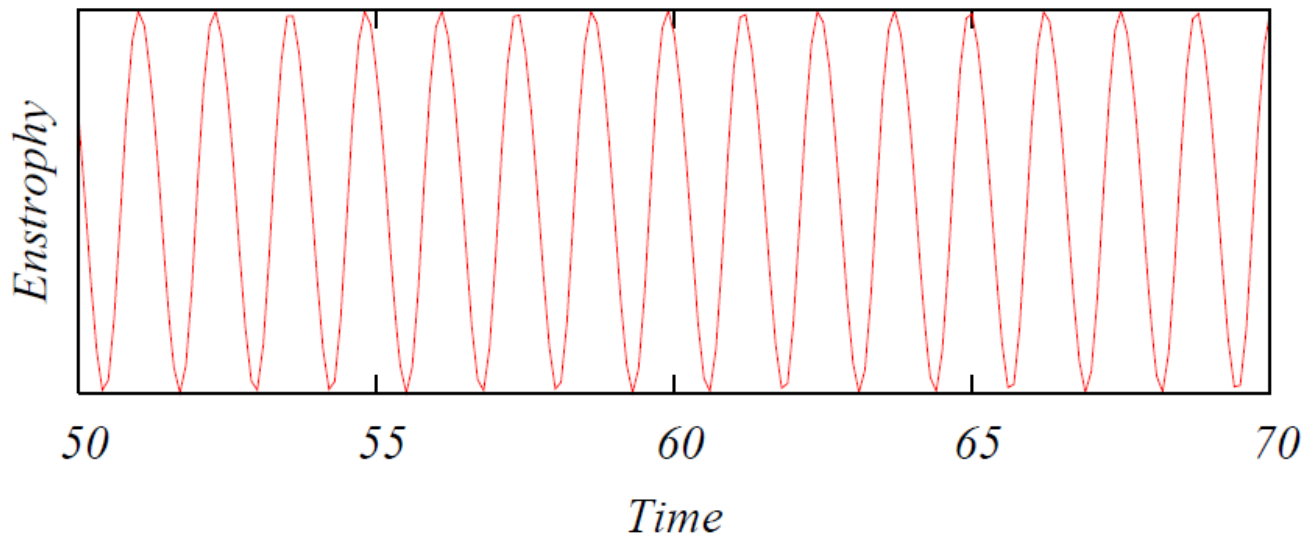
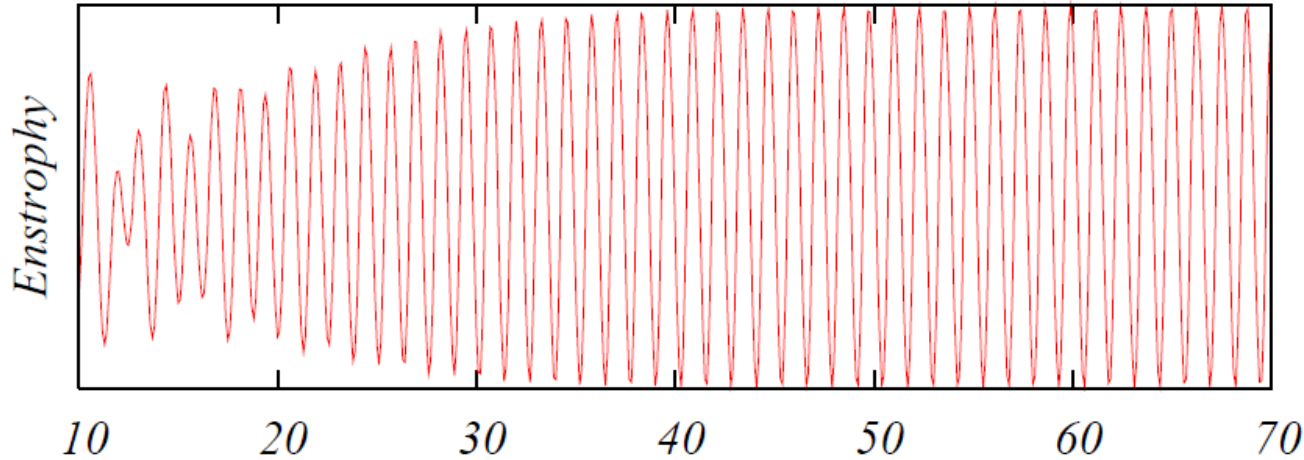
$$\gamma = 0.2$$



$$\lambda = 5.0$$

$$\lambda = 0.10$$

Time-Series of Enstrophy



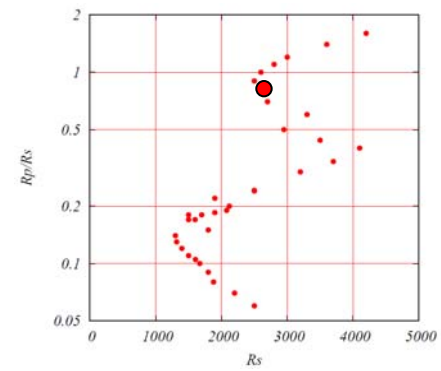
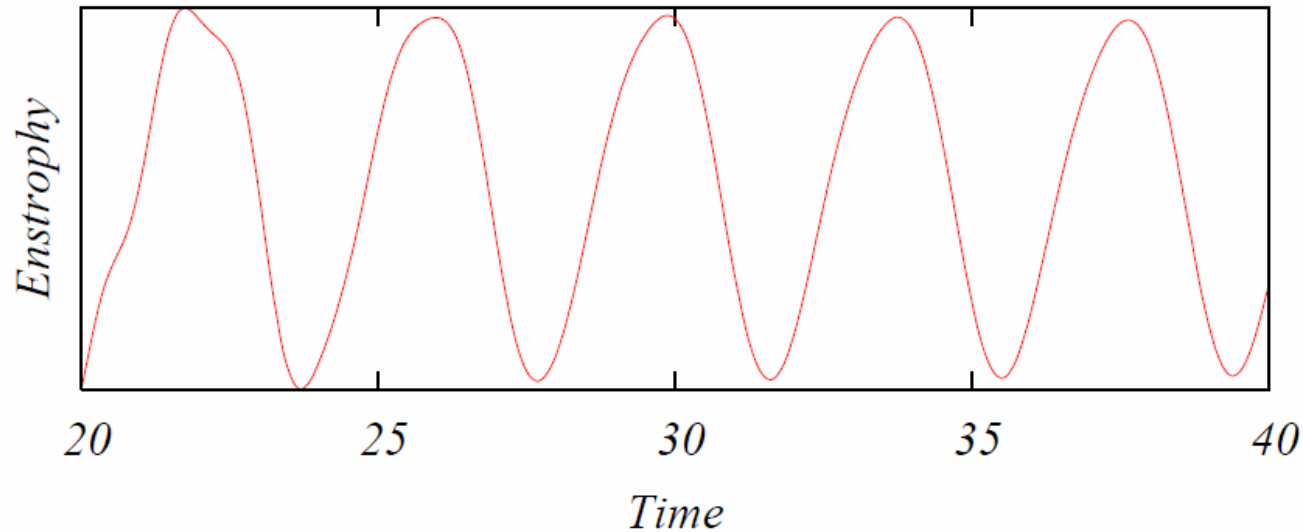
$$R_s = 2950$$

$$R_p = 1475$$

$$\gamma = 0.5$$

$$\lambda = 1.27$$

Time-Series of Enstrophy



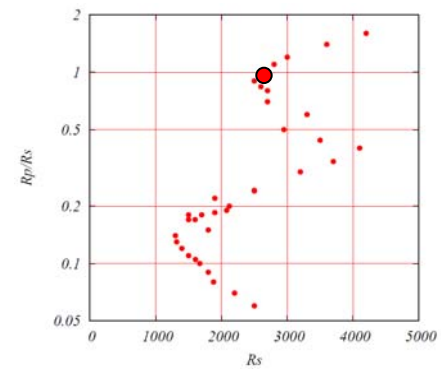
$$R_s = 2700$$

$$R_p = 2160$$

$$\gamma = 0.8$$

$$\lambda = 3.94$$

Time-Series of Enstrophy

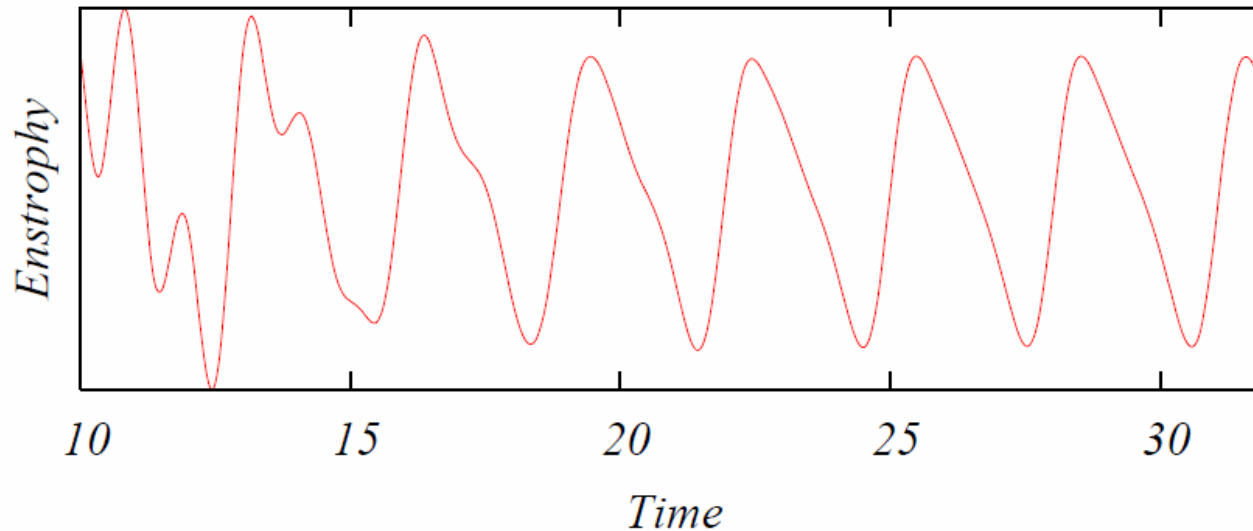


$$R_s = 2600$$

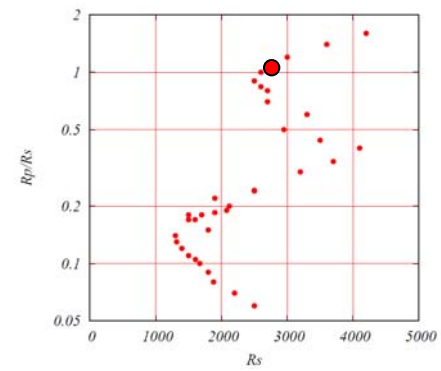
$$R_p = 2600$$

$$\gamma = 1$$

$$\lambda = 2.79$$



Time-Series of Enstrophy

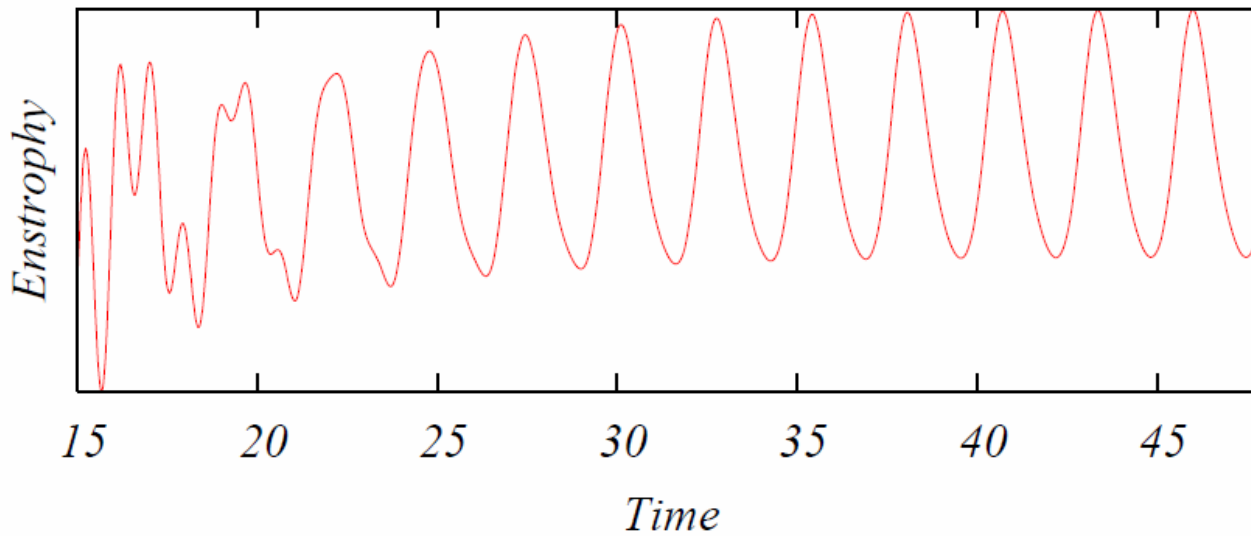


$$R_s = 2800$$

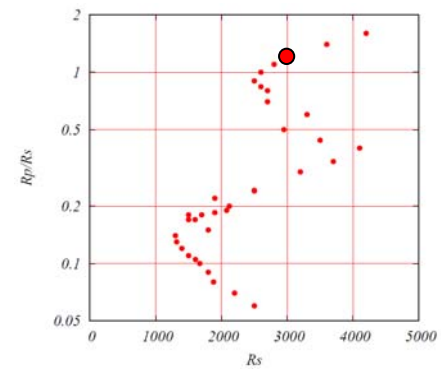
$$R_p = 3080$$

$$\gamma = 1.1$$

$$\lambda = 2.64$$



Time-Series of Enstrophy

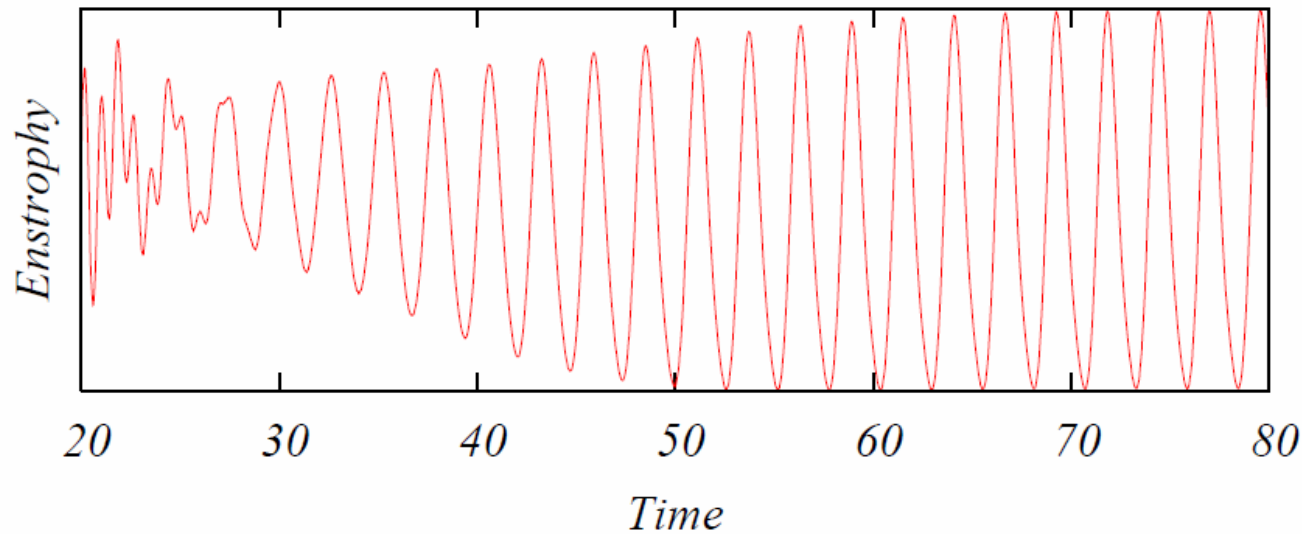


$$R_s = 3000$$

$$R_v = 3600$$

$$\gamma = 1.2$$

$$\lambda = 2.58$$



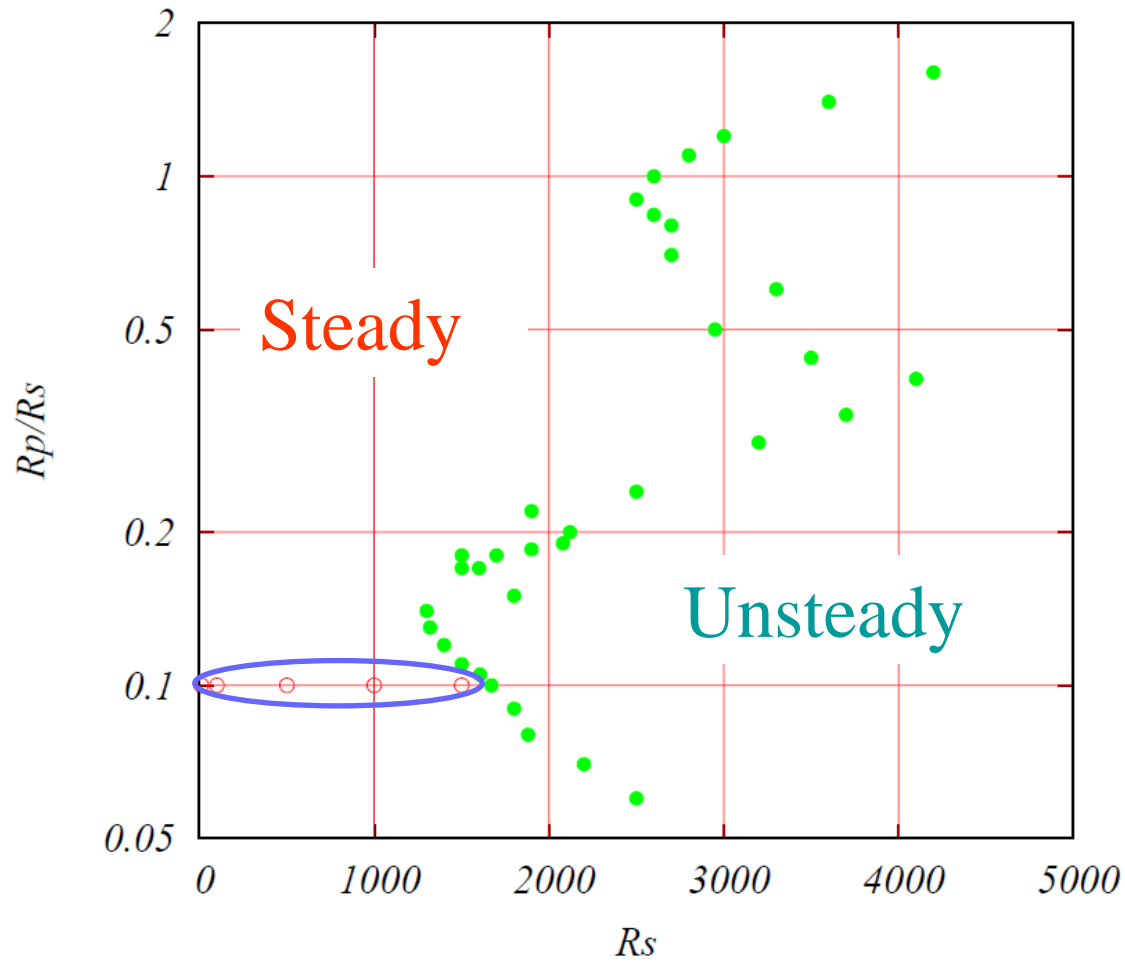
Outline

- 1 . Introduction
- 2 . Experiment – State Diagram
- 3 . Numerical Simulation – Stability boundary
Flow Structure
- 4 . Asymptotic Analysis – Flow Structure
- 5 . Summary

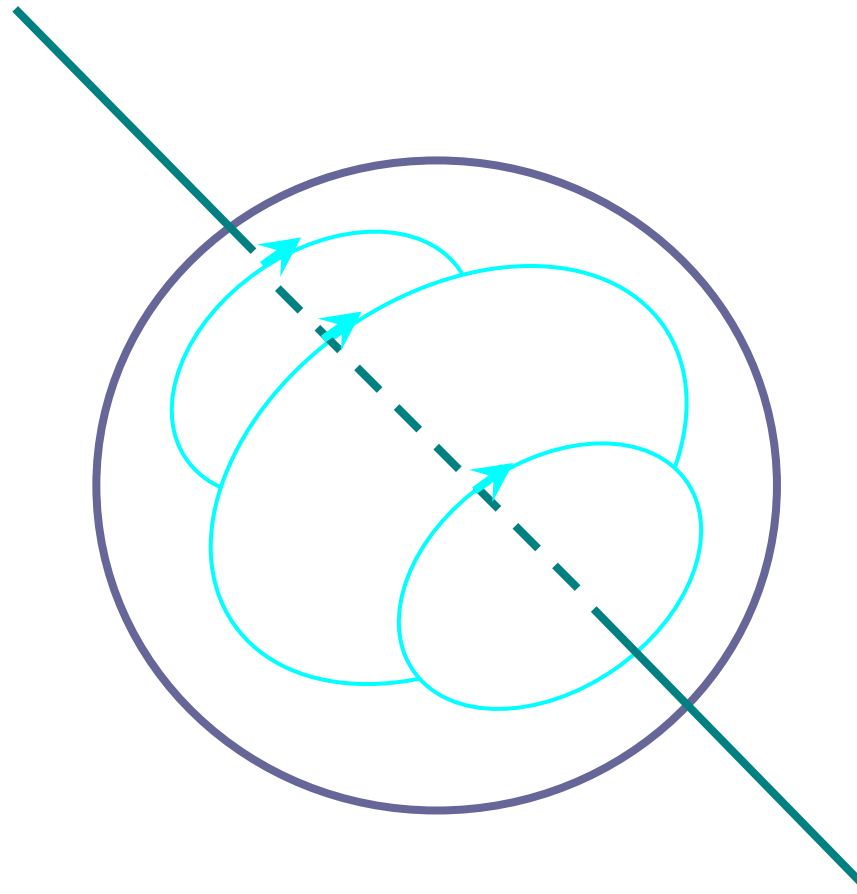
Flow Structure

Steady States

Stability Curve



Solid-Body Rotation



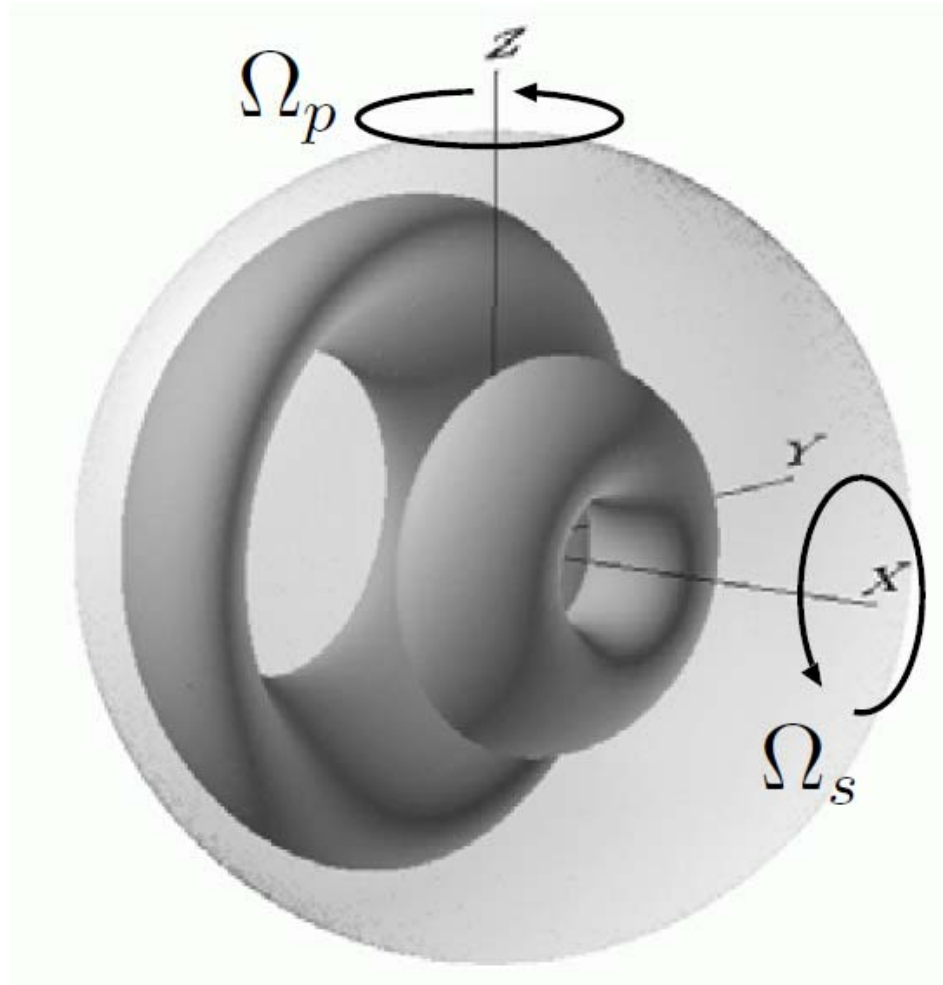
$$\Gamma \ll 1$$

or

$$Re \ll 1$$

Spin axis

Streamline Tori

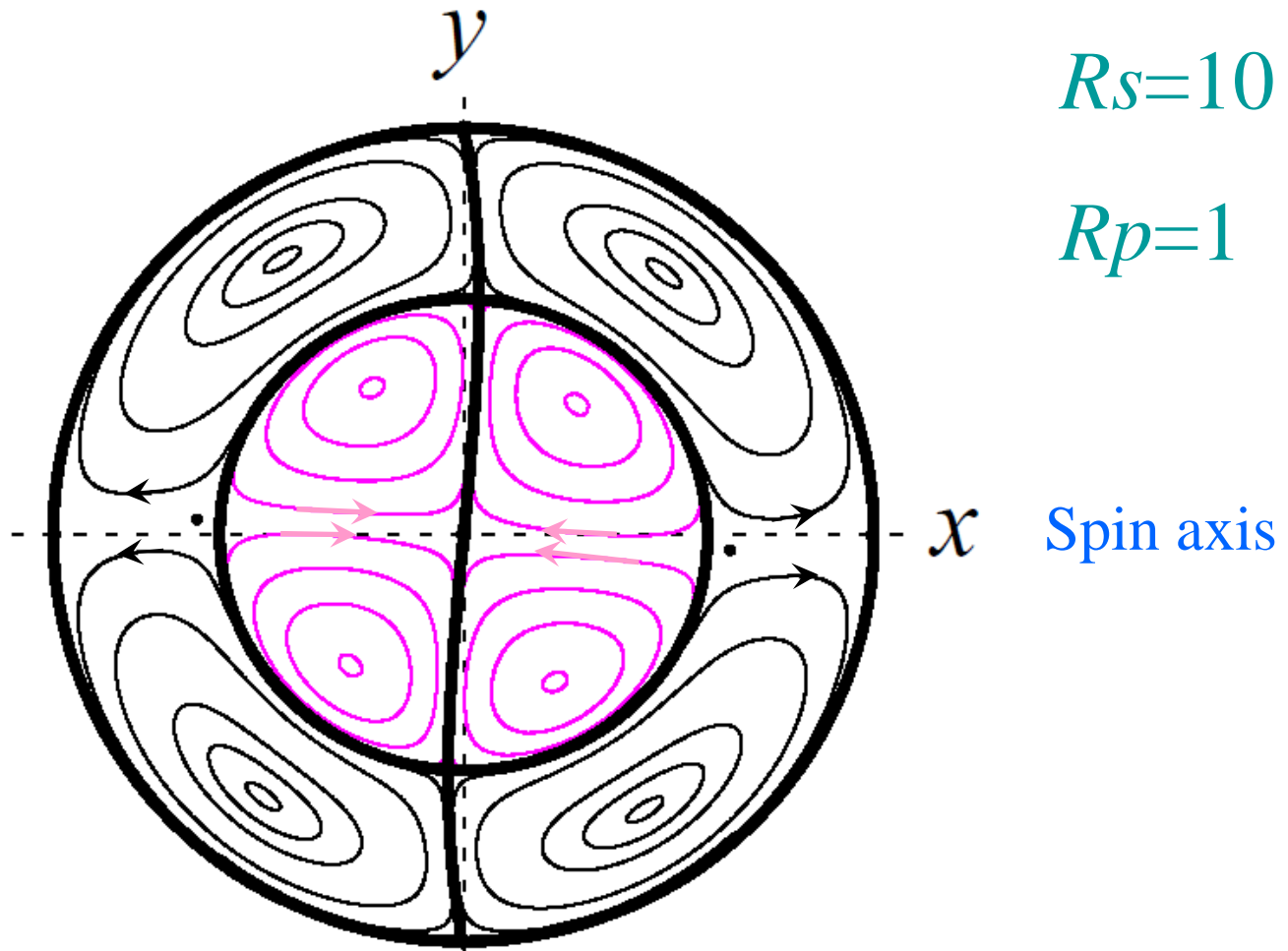


$$R_s=10$$

$$R_p=1$$

The whole surface of a torus is covered by a single streamline.

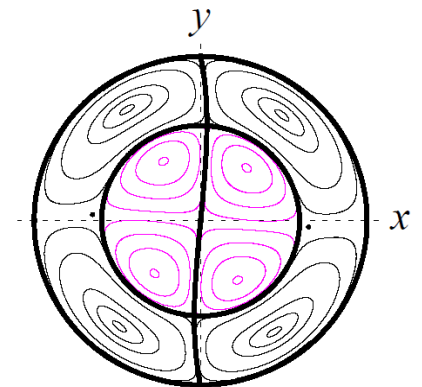
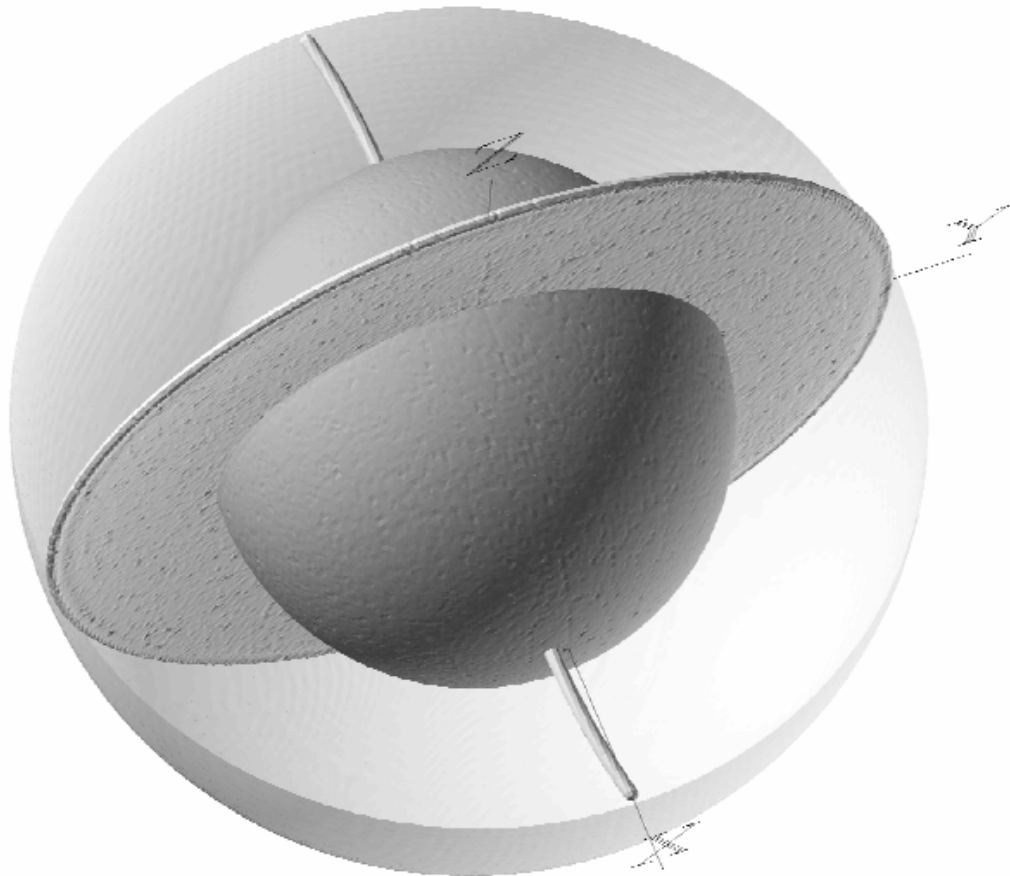
Cross-Section of Streamline Tori



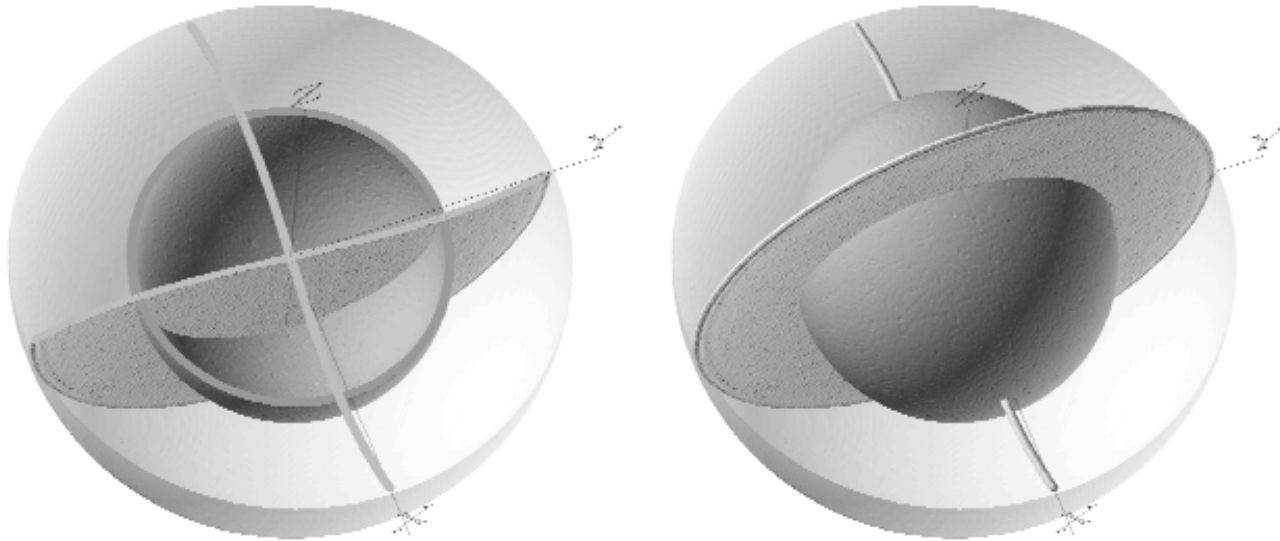
Separatrix Surfaces

$$R_s=10$$

$$R_p=1$$



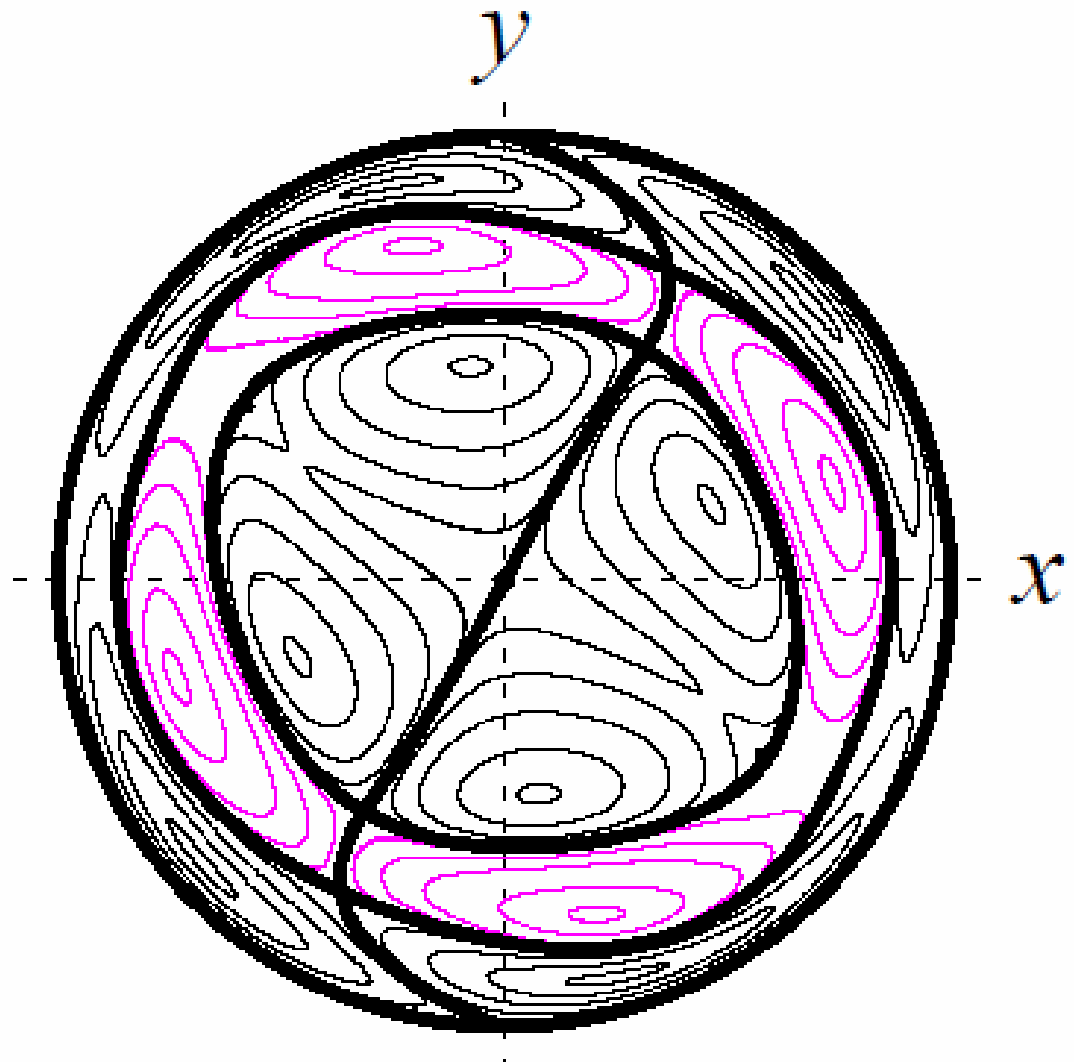
Separatrix Surfaces



$$R_s=10$$

$$R_p=1$$

Cross-Section of Streamline Tori

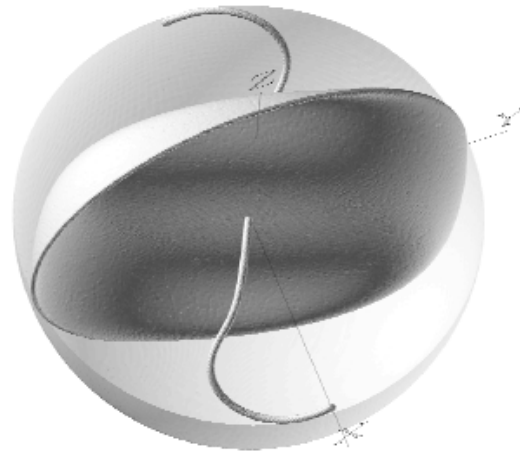
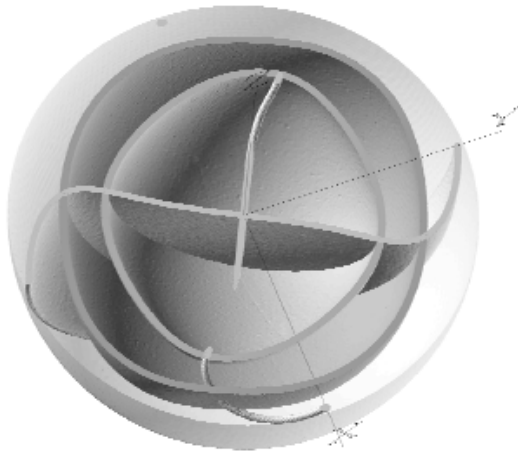


$R_s=200$

$R_p=20$

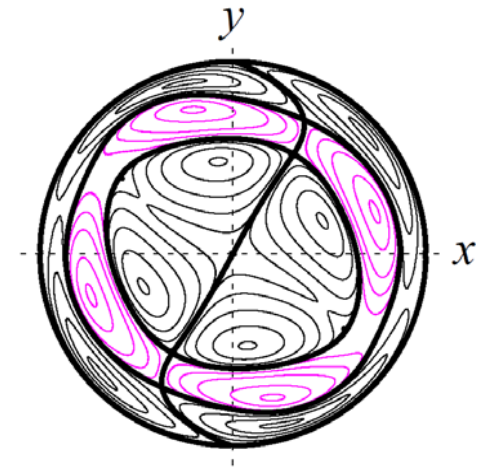
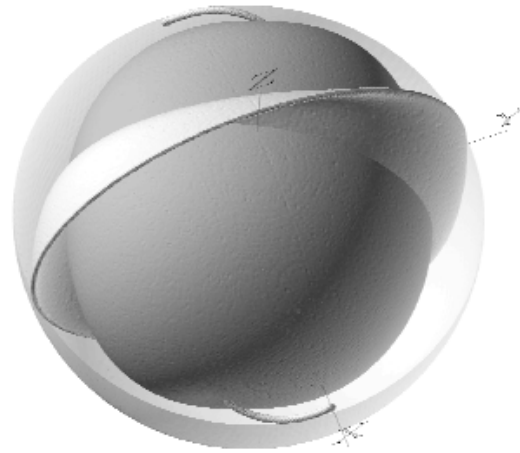
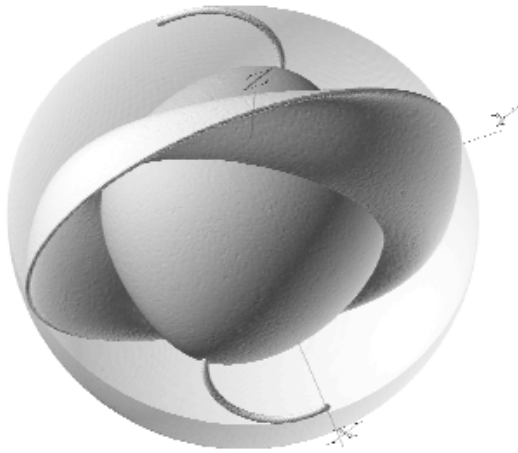
x Spin axis

Separatrix Surfaces

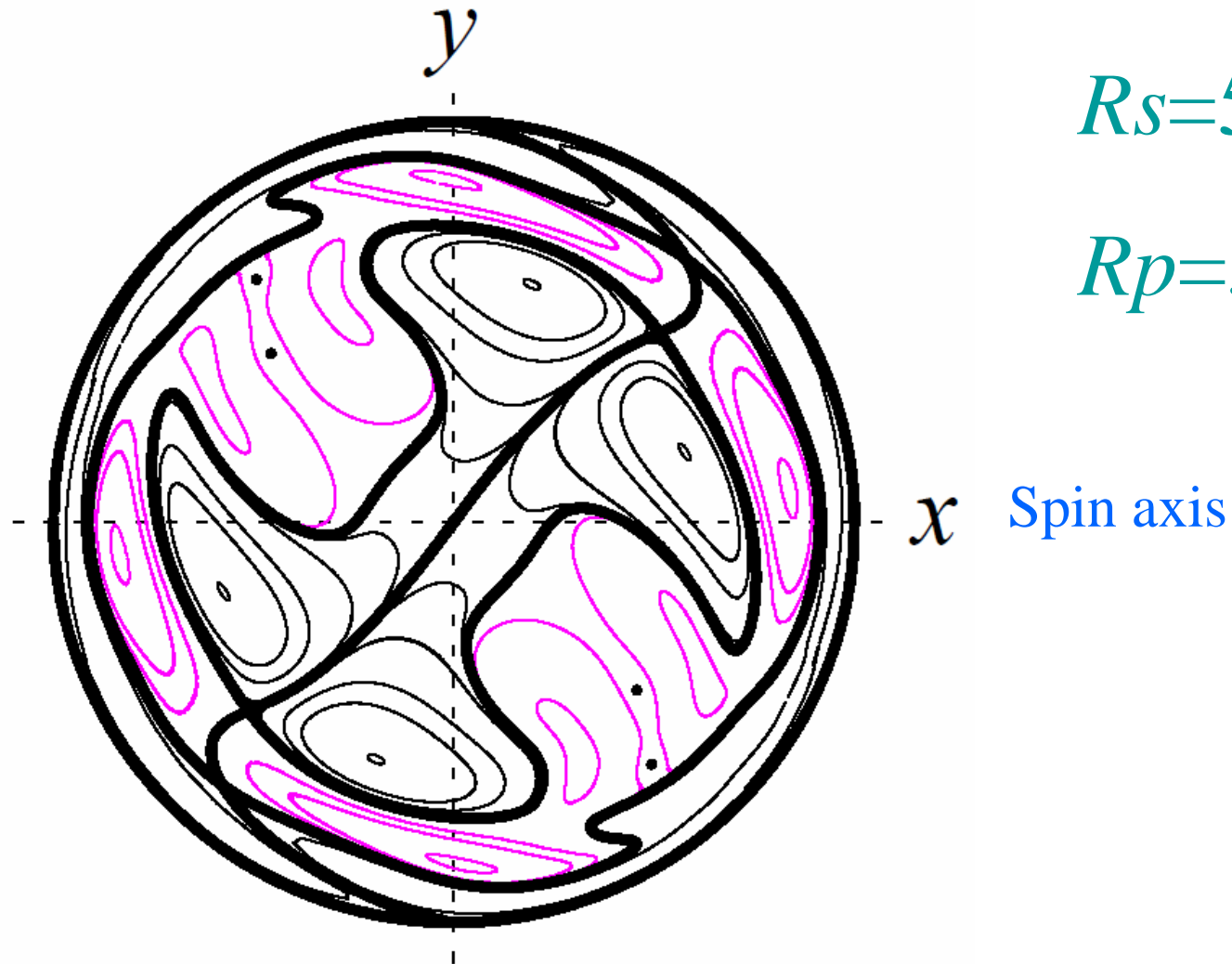


$R_s=200$

$R_p=20$



Cross-Section of Streamline Tori

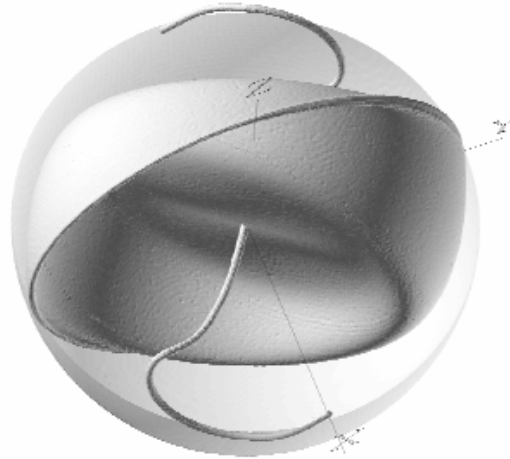
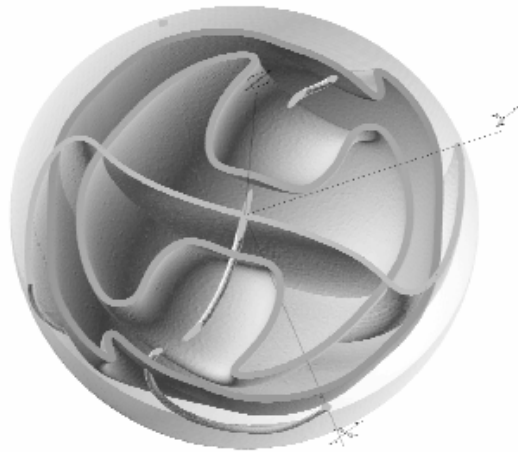


$$R_s=500$$

$$R_p=50$$

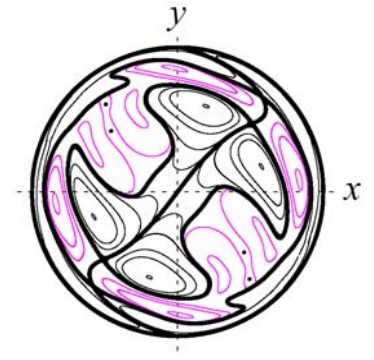
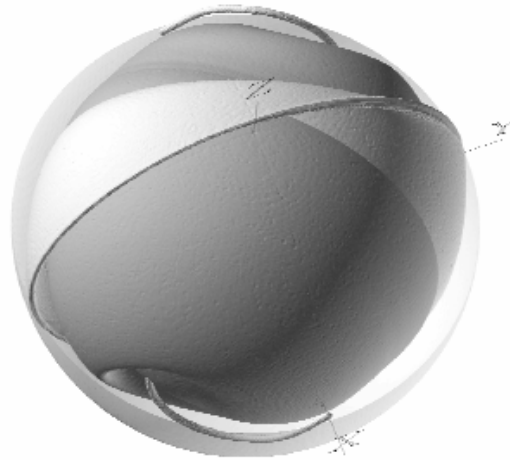
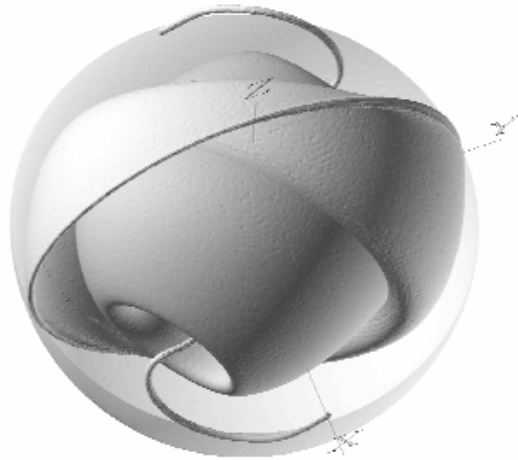
x Spin axis

Separatrix Surfaces

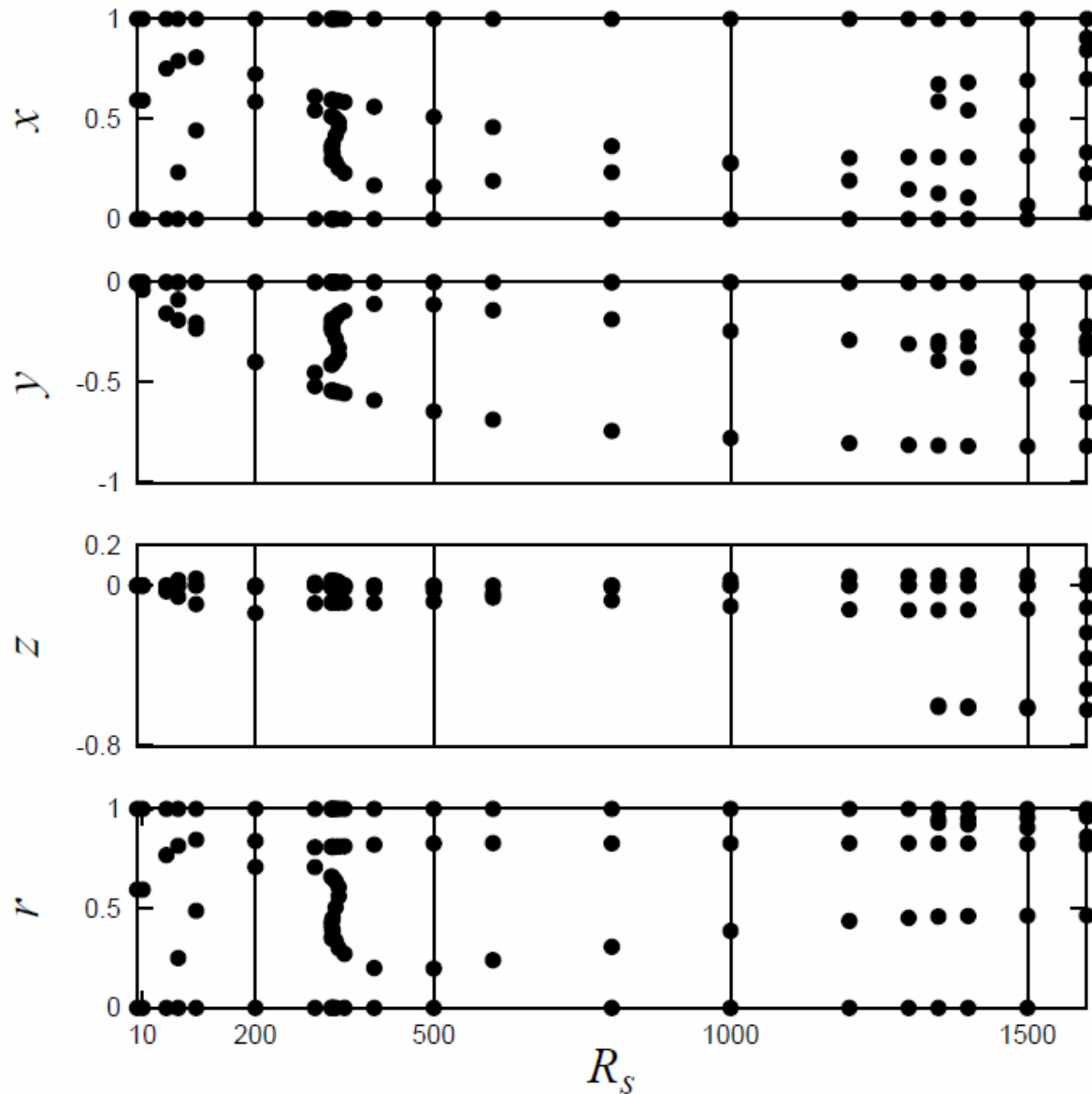


$R_s=500$

$R_p=50$



Location of Stagnation Points



Outline

- 1 . Introduction
- 2 . Experiment – State Diagram
- 3 . Numerical Simulation – Stability boundary
Flow Structure
- 4 . Asymptotic Analysis – Flow Structure
- 5 . Summary

Asymptotic Analysis

In the double limit of
small Reynolds numbers
and large times

Low-Reynolds-Number Flow

$$R_s \frac{\partial \mathbf{u}}{\partial t} = R_s \mathbf{u} \times \boldsymbol{\omega} - 2\Gamma R_s \hat{\mathbf{z}} \times \mathbf{u} - R_s \nabla P + \nabla^2 \mathbf{u}$$

$$P = p + \frac{1}{2} |\mathbf{u}|^2 + \frac{1}{2} \Gamma^2 (\mathbf{r} \times \hat{\mathbf{z}})^2$$

$$\Gamma = \frac{R_p}{R_s} = \frac{\Omega_p}{\Omega_s} = O(1)$$

$$R_s \ll 1 \quad R_p \ll 1$$

$$\mathbf{u} = \mathbf{u}^{(0)} + R_s \mathbf{u}^{(1)} + R_s^2 \mathbf{u}^{(2)} + \dots,$$

$$\boldsymbol{\omega} = \boldsymbol{\omega}^{(0)} + R_s \boldsymbol{\omega}^{(1)} + R_s^2 \boldsymbol{\omega}^{(2)} + \dots,$$

$$P = P^{(0)} + R_s P^{(1)} + R_s^2 P^{(2)} + \dots$$

Low-Reynolds-Number Flow

0th Order

$$u_r^{(0)} = 0,$$

$$u_\theta^{(0)} = 0,$$

$$u_\varphi^{(0)} = r \sin \theta, \quad \text{Solid-body rotation}$$

1st Order

$$u_r^{(1)} = 0,$$

$$u_\theta^{(1)} = \frac{\Gamma}{10} (1 - r^2) r \sin \varphi,$$

$$u_\varphi^{(1)} = \frac{\Gamma}{10} (1 - r^2) r \cos \theta \cos \varphi,$$

Differential rotation around y-axis

Low-Reynolds-Number Flow

2nd Order

$$u_r^{(2)} = \frac{\Gamma}{420} r(1 - r^2)^2 \sin \theta \cos \varphi (\Gamma \sin \theta \sin \varphi + \cos \theta),$$

$$u_\theta^{(2)} = -\frac{\Gamma}{2520} r(7r^2 - 3)(1 - r^2)(\Gamma \sin 2\theta \sin \varphi + \cos 2\theta) \cos \varphi,$$

$$u_\varphi^{(2)} = -\frac{\Gamma}{2520} r(7r^2 - 3)(1 - r^2)(\Gamma \sin \theta \cos 2\varphi - \cos \theta \sin \varphi)$$

$$-\frac{\Gamma^2}{1400} r(9 - 5r^2)(1 - r^2) \sin \theta$$

Low-Reynolds-Number Flow

3rd Order

$$u_r^{(3)} = \left[\frac{\Gamma^3(58 - 15r^2)}{623700} + \frac{\Gamma(5 - 3r^2)}{249480} \right] r(1 - r^2)^2 \sin 2\theta \sin \varphi$$
$$+ \frac{\Gamma^2(10 - 3r^2)r(1 - r^2)^2}{113400} (3 \cos^2 \theta - 1)$$
$$- \frac{\Gamma^2(148 - 69r^2)r(1 - r^2)^2}{1247400} \sin^2 \theta \cos 2\varphi,$$

Low-Reynolds-Number Flow

3rd Order

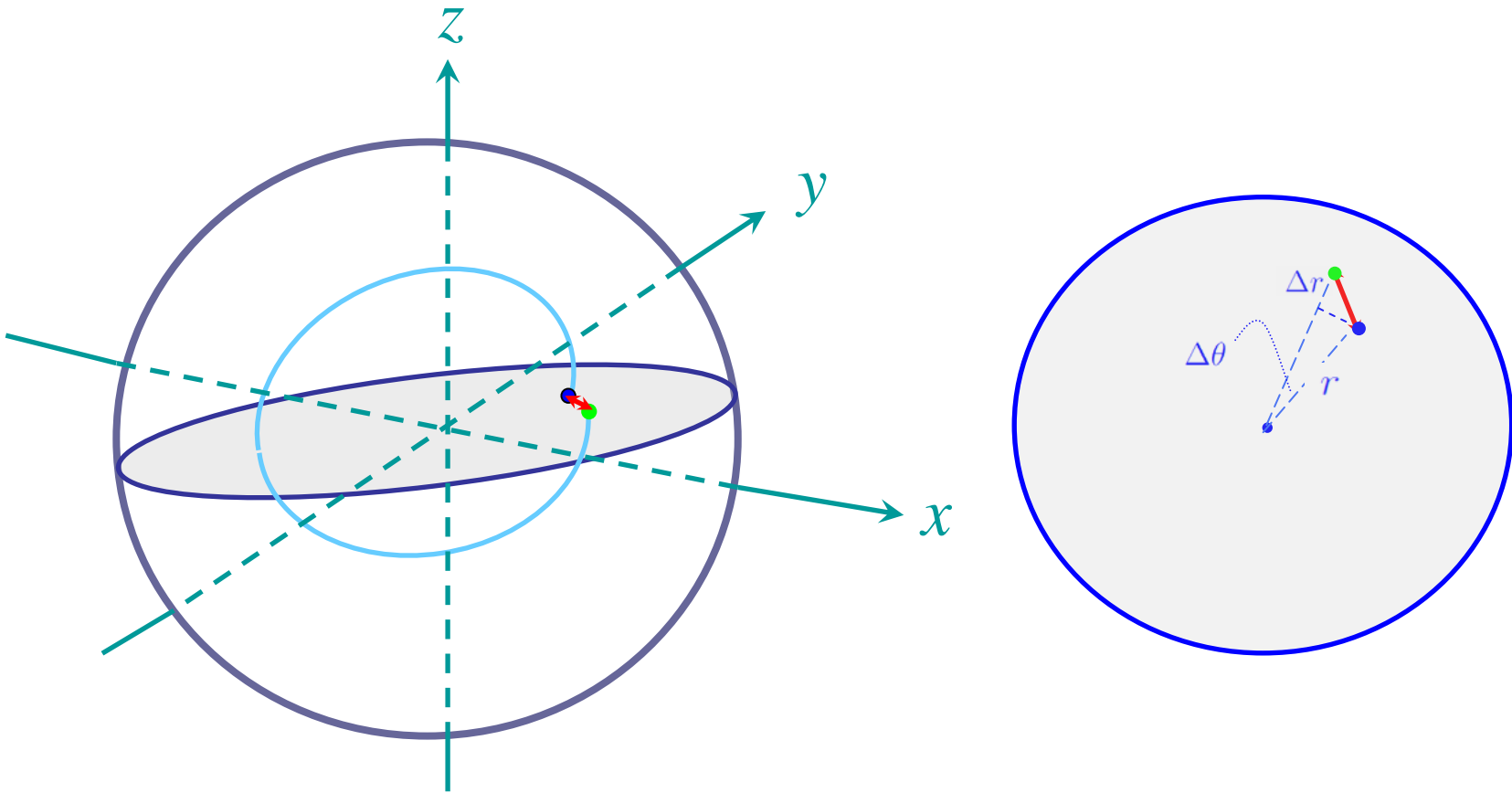
$$\begin{aligned}u_{\theta}^{(3)} = & -\frac{\Gamma^3}{249480}r^3(1-r^2)(13-9r^2)\sin^2\theta\sin 3\varphi \\ & -\frac{\Gamma^3}{12474000}r(1-r^2)(4884-4555r^2+1275r^4)\sin\varphi \\ & +\frac{\Gamma^3}{2494800}r(1-r^2)(232-663r^2+195r^4)\cos 2\theta\sin\varphi \\ & -\frac{\Gamma^2}{2494800}r(1-r^2)(148-287r^2+87r^4)\sin 2\theta\cos 2\varphi \\ & -\frac{\Gamma^2}{226800}r(1-r^2)(30-85r^2+27r^4)\sin 2\theta \\ & -\frac{\Gamma}{2494800}r(1-r^2)(99-250r^2+135r^4)\sin\varphi \\ & +\frac{\Gamma}{249480}r(1-r^2)^2(5-3r^2)\cos 2\theta\sin\varphi,\end{aligned}$$

Low-Reynolds-Number Flow

3rd Order

$$\begin{aligned}u_{\varphi}^{(3)} = & -\frac{\Gamma^3}{249480}r^3(1-r^2)(13-9r^2)\sin^2\theta\cos\theta\cos 3\varphi \\ & -\frac{\Gamma^3}{997920}r^3(1-r^2)(13-9r^2)\cos 3\theta\cos\varphi \\ & -\frac{\Gamma^3}{24948000}r(1-r^2)(7448-2805r^2+825r^4)\cos\theta\cos\varphi \\ & +\frac{\Gamma^2}{249480}r^3(1-r^2)(13-9r^2)\sin 3\theta\sin 2\varphi \\ & +\frac{\Gamma^2}{623700}r(1-r^2)(74-241r^2+111r^4)\sin\theta\sin 2\varphi \\ & +\frac{\Gamma}{249480}r^3(1-r^2)(13-9r^2)\cos 3\theta\cos\varphi \\ & -\frac{\Gamma}{2494800}r(1-r^2)(49-40r^2+15r^4)\cos\theta\cos\varphi.\end{aligned}$$

Poincare Map of Streamline



$$\Delta r = -R_s^3 \frac{\pi \Gamma^2}{16200} r_0 (1 - r_0^2)^2 (1 - 3r_0^2) (3 \cos^2 \theta_0 - 1) + O(R_s^4)$$

$$\Delta \theta = R_s^3 \frac{\pi \Gamma^2}{32400} (1 - r_0^2) (3 - 22r_0^2 + 27r_0^4) \sin 2\theta_0 + O(R_s^4)$$

Cross-Section of a Streamline Torus

$$\frac{dr}{d\theta} = -\frac{2r(1-r^2)(1-3r^2)(3\cos^2\theta-1)}{(3-22r^2+27r^4)\sin 2\theta}$$

$$R_s \ll 1$$

$$R_p \ll 1$$

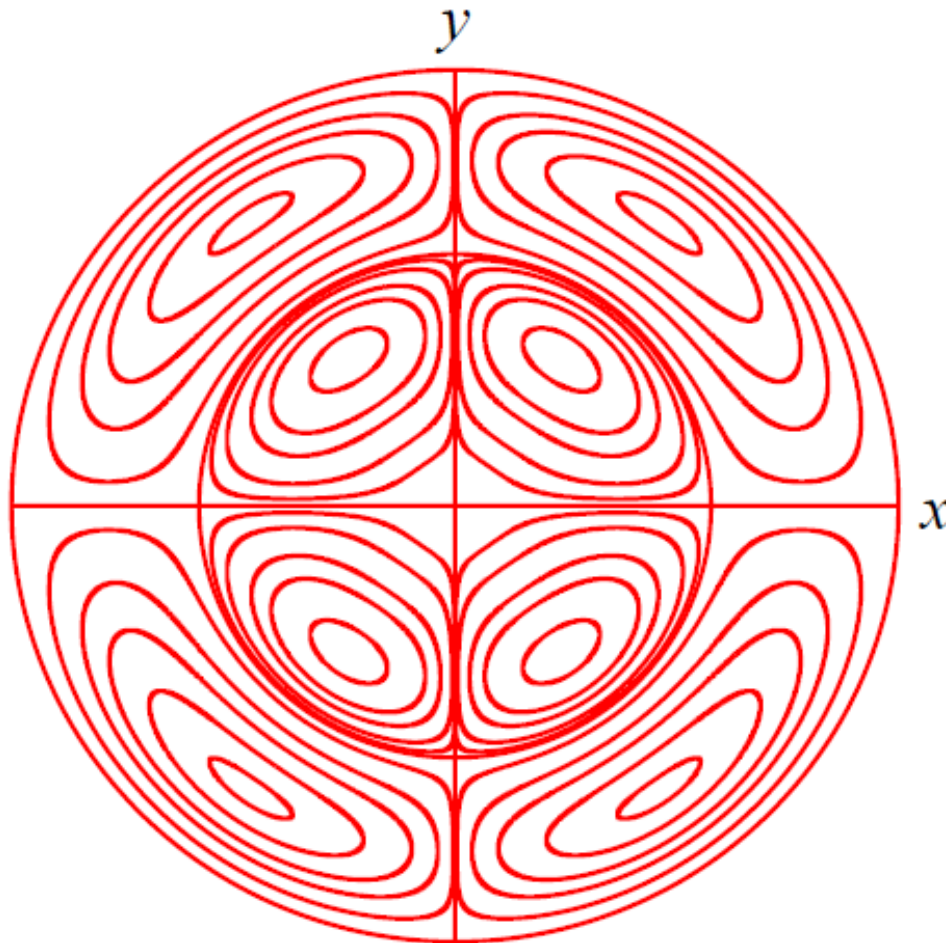
$$t = O(R_s R_p^2)$$

$$r_0 \rightarrow r, \theta_0 \rightarrow \theta, \Delta r / \Delta \theta \rightarrow dr / d\theta$$

$$r^3(1-r^2)^2\left(\frac{1}{3}-r^2\right)(1-\cos^2\theta)\cos\theta = \text{const.}$$

$$(1-x^2-y^2-z^2)^2\left(\frac{1}{3}-x^2-y^2-z^2\right)(y^2+z^2)x = \text{const.}$$

Cross-Section of a Streamline Torus



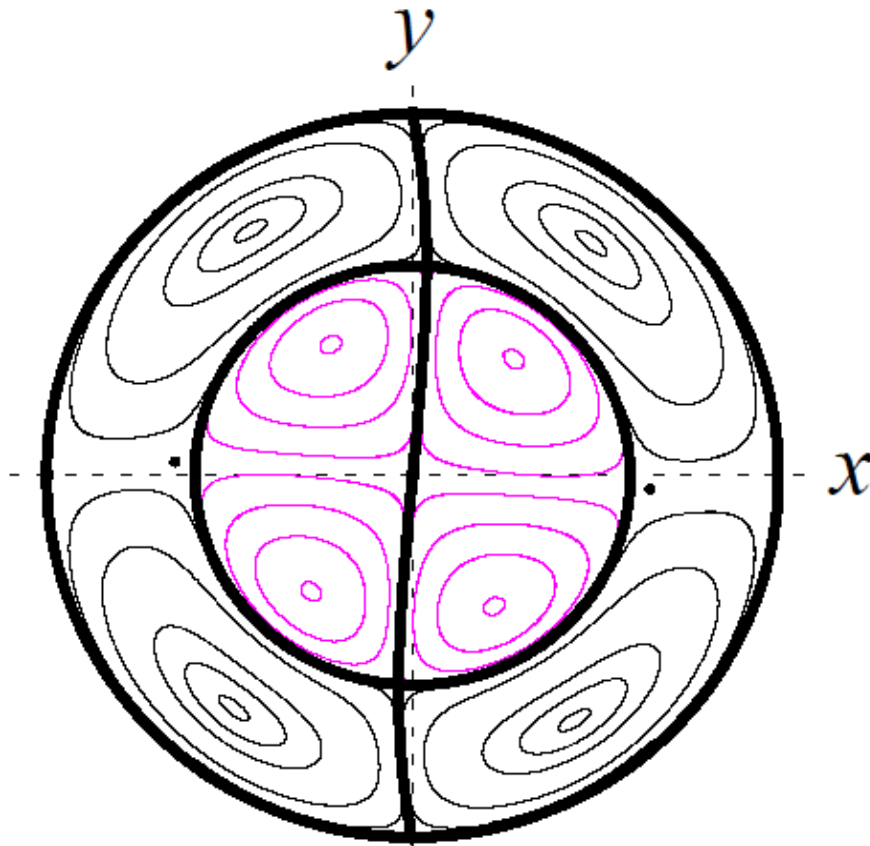
$$R_s \ll 1$$

$$R_p \ll 1$$

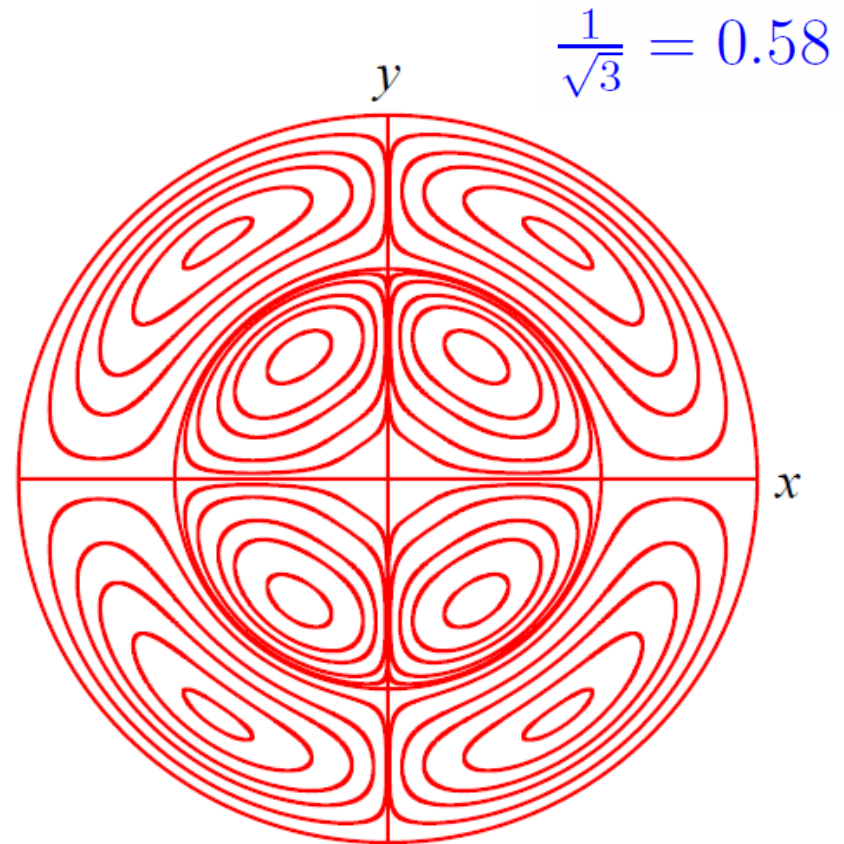
$$t = O(R_s R_p^2)$$

$$r^3(1 - r^2)^2\left(\frac{1}{3} - r^2\right)(1 - \cos^2 \theta) \cos \theta = \text{const.}$$

Comparison: DNS & Theory



$R_s=10, R_p=1$



$$\frac{1}{\sqrt{3}} = 0.58$$

$$r^3(1-r^2)^2\left(\frac{1}{3}-r^2\right)(1-\cos^2\theta)\cos\theta = \text{const.}$$

Summary

- ① The state diagram of flows in a precessing sphere was constructed experimentally.
- ② The stability curve of steady flow was revealed partially by DNS.
- ③ The toral structure of streamlines was observed by DNS. So far no chaotic streamline has been found.
- ④ An analytical expression was obtained for the streamline tori in the double limit of small Reynolds numbers and large times.

Future Problems

- ① Complete the stability curve
- ② Clarify the characteristics of critical modes
- ③ Perform the linear stability analysis
- ④ Raise the speed of the numerical code
- ⑤ Examine the turbulence characteristics, such as intensity, mixing, etc.